Tomas Bata University in Zlín
Centre of Polymer Systems

Doctoral Thesis Summary

Intelligent Electrorheological Fluids

Inteligentní elektroreologické tekutiny

Author: Ing. Erika Kutálková , Ph.D.

Degree program: P3972 Nanotechnology and Advanced Materials

Degree course: 3942V006 Nanotechnology and Advanced Materials

Supervisor: doc. Ing. Michal Sedlačík, Ph.D.

Consultants: Ing. Miroslav Mrlík, Ph.D.

                  Ing. Tomáš Plachý, Ph.D.

Reviewers: doc. Dr. Ing. Vladimír Pavlínek, Ph.D.

                  prof. Ing. Petr Slobodian, Ph.D.

Zlín, August 2021

ACKNOWLEDGMENT

ABSTRACT

In recent years, so-called intelligent fluids form a significant target of focus of the development of the industry and many scientific groups, as they seem to be very auspicious material of the future due to their unique properties when an external stimuli, such as an electric field, is applied. Electrorheological fluids have already been widely utilized, especially as vibration damping devices in mechanical engineering and medicine.

However, there are still several issues that limit their application in everyday life. Some of the current electrorheological materials demonstrate rapid sedimentation of dispersed particles and achieve insignificant electrorheological performance. Therefore, this thesis is focused on preparing and investigating suitable materials to improve sedimentation stability as well as the electrorheological effect of such fluids. It is necessary to find a required balance between excellent sedimentation stability and electrorheological performance that corresponds with the intended application. Morphology, size, electrical conductivity, and other properties of the particles influence overall the system's behavior. Thus, the previously mentioned issues above can be eliminated by modifying some of these factors and are properly discussed in this thesis.

ABSTRAKT

Vývoj průmyslu a mnoho vědeckých skupin se v posledních letech stále více zaměřuje na tzv. inteligentní tekutiny. Ukazují se býti velmi slibnými materiály budoucnosti díky svým jedinečným vlastnostem, kterých dosahují vlivem vnějšího podnětu, např. elektrickým polem. Elektroreologické tekutiny jsou již navrženy, zejména jako zařízení pro tlumení vibrací ve strojírenství a medicíně.

Stále však existuje několik problémů, které omezují jejich použití v každodenním životě. Některé ze současných elektroreologických tekutin vykazují výraznou sedimentaci rozptýlených částic a nedosahují významných elektrorheologických efektů. Tato práce je proto zaměřena na přípravu a zkoumání vhodných materiálů, které by zlepšily sedimentační stabilitu a elektroreologický účinek těchto tekutin. Vždy je nezbytné najít rovnováhu mezi vynikající sedimentační stabilitou a elektroreologickým výkonem, což souvisí se zamýšlenou aplikací. Morfologie, velikost, elektrická vodivost a další vlastnosti částic ovlivňují celkové chování systému, a proto lze výše zmíněné problémy eliminovat úpravou některých z těchto faktorů, což je důkladně popsáno v této práci.

CONTENT

1. THEORETICAL BACKGROUND

1.1 Introduction to Electrorheology

Nowadays, with a continuous growth of scientific interest, intelligent materials are widely used in many areas of industrial engineering. These unique types of materials are called intelligent as a result of the changes in their physical properties upon the application of an external stimulus, for instance, pH [1], temperature [2], UV light [3] , electric or magnetic field [4], etc.

Electrorheological fluids (ERFs), firstly discovered by Winslow in 1948 [5], are known as fascinating smart materials which can precisely control their rheological parameters by means of an external electric field. These materials are generally called suspensions consisting of solid particles as dispersed phase and liquid medium as continuous phase. The dispersed phase is composed of electrically polarizable particles, while the liquid continuous phase is usually an insulating non-polar medium. The external electric field plays an important role. In the absence of the external electric field, the particles are randomly distributed in the liquid medium (Fig. 1a) and the system exhibits nearly Newtonian behavior. However, with the application of an electric field, the particles in the suspension start to form highly organized chain-like structures due to dipole–dipole interactions between the particles aligned along the external electric field strength (Fig. 1b). Thus, their unique ability lies in a reversible transition from a liquid to a solid-like state within several milliseconds. This mechanism leads to a substantial change in rheological properties including increased viscosity, shear stress, and viscoelastic moduli. As a result of this phenomenon called electrorheological (ER) effect, the ERFs are highly desired in many industrial applications including electromechanical devices, such as human muscle stimulators, medical haptic devices, hydraulic valves and clutches [6], engine mounts, torque transducers, and various hydraulic dampers [7-9].

Electrorheological performance is affected by a number of parameters including the strength of the electric field, the volume fraction of particles, their morphology, size, and electrical conductivity [8, 10]. Generally, the geometry of the particle plays a considerable role in ER response. One-dimensional (1D) and two-dimensional (2D) particles, such as rod-like particles, display a more robust internal structures and enhanced yield stress when compared to spherical [4, 11, 12]. The effect occurs due to much higher dipole-dipole interparticle attractive forces which are a result of the side-by-side major axis (higher aspect ratio) connection of particles (Fig. 1c) and thus higher solid friction between them [12, 13].
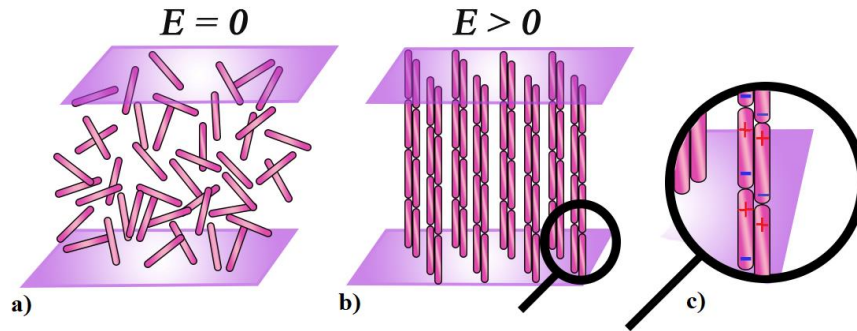
Fig. 1. Microstructure of electrically polarizable 1D particles dispersed in an ER fluid in the absence (a), and in the presence of an electric field (b), when internal structures are created due to dipole-dipole interactions (c). Redrawn from Wu et al. [14].

1.2 The Electrorheological Materials

1.2.1 Liquid Continuous Phase

The liquid medium has to fulfill certain criteria to be suitable for continuous phase in electrorheology. Thus, the most common liquid medium for ERFs is a non-conductive oil with a low relative permittivity. Electrorheological performance of prepared ERFs can be influenced by different terminal groups of used non-conductive oil, such as hydroxyl, hydrogen, and methyl, which otherwise have very similar viscosity [15]. The interaction between the liquid medium and solid particles, significantly influence the ER effect and the ER efficiency [16]. Ideal properties should include high boiling point and low solidifying point to ensure smooth operation within a certain working temperature range without any evaporation of the suspension. In addition, the oil should have a low viscosity to maintain the viscosity of the whole ER system at desired values when the electric field is switched off, and with lower oil viscosity the ER efficiency should rise [17]. Furthermore, the oil should have a density close to that of the dispersed particles to prevent particles sedimentation, high chemical, thermal and thermo-oxidative stability. The compatibility with particles used is also notably important as well. Last but not least, the liquid medium should have low toxicity and some hydrophobicity for avoiding the absorption of water from the environment. Therefore, silicone or mineral oils represent the most commonly used material as a liquid continuous phase nowadays, however, it is also possible to choose vegetable oil, paraffin, kerosene, chlorinated hydrocarbon, etc. depending on the properties required in the desired application [16, 18].

1.2.2 Dispersed Phase

Dispersed phase must also meet certain criteria for use in ERFs for real applications. Usually, solid particles have to be semiconducting or electrically polarizable in order to form internal chain structures in prepared ERF as a result

7

of interactions between particles upon the application of the external electric field [19]. The particles can be divided into two main groups, namely inorganic and organic.

Inorganic Materials

One of the most investigated materials are inorganic oxide materials. Some of the metallic oxides [20-22] or ceramic materials [23] have been used for highly efficient ERFs. Continuous development in silica [24-27], titanates [12, 28-33], clay materials [34, 35], or iron oxides [36, 37] appears to be promising for obtaining an ER-effective dispersed phase. In recent years, titanates, in particular, have been in the spotlight as a very promising material for use in electrorheology. This inorganic material exhibits enhanced ER performance with high yield stresses rather due to its high relative permittivity than the conductivity of the particles [29, 38]. Unfortunately, the major disadvantages of all these inorganic materials are their high viscosity in the off-state, and high density resulting in fast sedimentation.

Organic Materials

Organic materials have been considered significantly more propitious than the inorganic ones. The dominant group of organic and polymeric materials is classified into two divisions, namely materials having conjugated π bonds and highly polarizable group on the molecular chain (hydroxyl, cyano, amido, etc.) [18]. The first group, with conjugated π bonds, are conducting polymers such as polyaniline (PANI) [39, 40], poly(diphenylamine) [41], polypyrrole (PPy) [42, 43], and their derivatives. These materials are widely used in electrorheology owing to their low density, excellent environmental stability, favorable production cost, easy synthesis, and controllable conductivity appearing to be crucial. The conductivity of the conjugated polymer can be tailored by a doping process or by controlling the carbonization temperature [18, 44].

The group of organic materials applicable as a dispersed phase in ERFs further includes oligomers of conducting polymers [45], various types of carbonaceous materials [46-48], and cellulose along with its derivates [49, 50].

Especially, aniline oligomers, represented by several aniline constitutional units linked together, have gained attention due to their semiconducting character. The oligomers have easier preparation in comparison with the vide supra mentioned conducting polymers while the suitable conductivity is provided through the inter-molecular charge transport [51, 52]. This mechanism allows the preparation of a material with controllable conductivity, thus generating high ER effect. On the other hand, biopolymers, which are renewable, biodegradable, and with favorable price, currently have also obtained substantial attention. Pure cellulose material is not attractive for preparing ERFs since it is sensitive to water and achieves a low ER effect [53]. Therefore, microcrystalline or microfibrillated

cellulose can be modified by e.g. using a urea-terminated silane [50] or a phosphate ester reaction [54].

1.3 Important Properties of Electrorheological Fluids

Electrorheological fluids display complicated flow characteristics, which have to be investigated in order to evaluate their suitability from a practical point of view. Rheological properties are determined under both cases, in the absence as well as in the presence of an electric field. Their dielectric properties and the conductivity of the particles also play a key role in ER performance.

1.3.1 Rheological Properties

Rheological parameters such as viscosity, yield stress, and viscoelastic moduli are significantly altered in a very short time (in order of a few milliseconds) when an external electric field is applied.

Steady-Shear Behavior

The yield stress (τ_y) which defines the rigidity of the created internal structures when an external field is applied belongs to significant properties of ERFs. Two types of τ_y can be distinguished, namely static, and dynamic yield stress. Static yield stress is defined as the upper-stress level of the pre-yield regime when the sample behaves as a solid substance without implying flow. The dynamic yield stress is described as the stress level at the beginning of the post-yield regime when the sample starts to flow at a very low shear rate [55]. Undoubtedly, to appropriately introduce these fluids into potential applications, an investigation of τ_y values using suitable rheological models is necessary [56].

Generally, in the absence of an external electric field, ERFs demonstrate Newtonian fluid behavior when the shear stresses increase linearly with increasing shear rate (Fig. 2), which is mathematically defined as a Newton model:

$$\tau = \eta \cdot \dot{\gamma} \tag{1}$$

where, τ is the shear stress, η and $\dot{\gamma}$ is the shear viscosity and the shear rate.

In contrast, in the presence of an external electric field, Bingham fluid behavior of the ERFs is observed. The values of τ_y are enhanced with the increase of external electric field owing to the formation of chain-like structures in the direction of the electric field (Eq. 2, Fig. 2). Bingham model is shown as follows [26, 57]:

$$\tau = \tau_y + \eta_{pl} \cdot \dot{\gamma}; \tau \geq \tau_y$$
$$\dot{\gamma} = 0; \tau < \tau_y \tag{2}$$

where η_{pl} is the plastic viscosity, $\dot{\gamma}$ is shear rate, τ_y and τ is the yield stress and the shear stress.

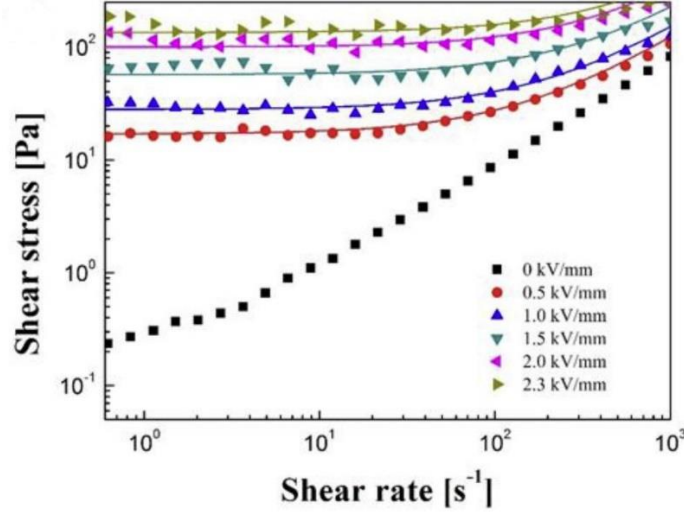*Fig. 2. Dependence of shear stress on the shear rate of silica/poly(o-anisidine) core–shell particle-based ERF (10 vol%) under different electric field strengths. Solid line is for Bingham model. Reprinted from Lee et al. [26].*

Although the Bingham model is one of the typical models for description of ERFs behavior in active state, i.e. when an external electric field is applied, the obtained τ_y values are inaccurate because the model does not operate at too low shear rates. Thus, τ cannot be fitted appropriately by the Bingham model for some ERFs [57]. For that reason, the Herschel–Bulkley model is frequently used as a more appropriate description of ERFs flow behavior:

$$\tau = \tau_y + K \cdot \dot{\gamma}^n; \tau \geq \tau_y \tag{3}$$

where τ_y and τ is the yield stress and the shear stress, respectively, K is the consistency index, and n is the flow index.

In the case of $n = 1$, consistency index is the post-yield viscosity and Herschel–Bulkley model is simplified to the Bingham model (Eq. 2). If the flow index is $n < 1$, the fluid shows a shear thinning behavior with the application of an external electric field. When the flow index is $n > 1$, the fluid behavior is evaluated as shear thickening [56, 58, 59].

Further, De Kee-Turcotte model has been used for the investigation of the rheological properties in various suspension systems including ERFs. Cho et al. have found that the values of τ_y and η obtained from Bingham model and De Kee–Turcotte are very alike [60]. The mathematic form of the De Kee–Turcotte model is given below via three-parameters model [60, 61]:

$$\tau = \tau_y + \eta_0 \cdot \dot{\gamma} e^{-t_1 \dot{\gamma}} \tag{4}$$

where τ_y and τ stands for the yield stress and the shear stress, η_0 is the shear viscosity for vanishing τ_y at the high shear rates, $\dot{\gamma}$ is shear rate, t_1 is a time constant.

Some of the ERFs do not exhibit typical shear stress plateau at low shear rates but an unusual decreasing trend of the shear stress can be observed (Fig. 3). The above-mentioned models are not able to fit effectively such a behavior. For that case, Cho–Choi–Jhon (CCJ) model has been proposed containing six parameters that correctly describe the ER flow behavior at a wide shear rate region. The CCJ model follows as [49, 62, 63]:

$$\tau = \frac{\tau_y}{1 + (t_1\dot{\gamma})^\alpha} + \eta_\infty \cdot \left(1 + \frac{1}{(t_2\dot{\gamma})^\beta}\right) \cdot \dot{\gamma} \qquad (5)$$

where the τ_y is the dynamic yield stress, the t_1 and t_2 are time constants describing the variation in shear stress. The exponent α is related to the decrease in the stress at low shear rates and the value of β is in a range of $0 - 1$, since $d\tau/d\dot{\gamma} > 0$, and the η_∞ represents shear viscosity at high shear rates.

As it appears in Fig. 3, at higher electric field strengths, the shear stress decreases with increasing shear rate, but from the certain critical shear rate values the shear stress starts to increase since hydrodynamic forces are stronger and dominate over electrostatic. Consequently, the internal organized structures are destroyed [63].
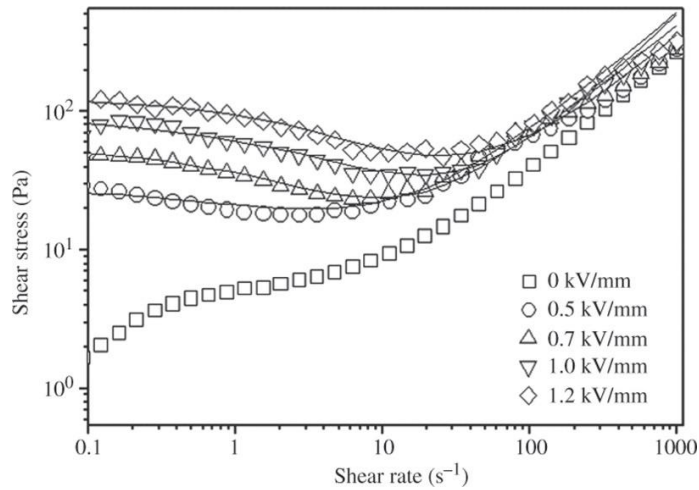

Fig. 3. Dependence of shear stress curves of PANI/clay-based ERF on the shear rate under different electric field strengths. Solid lines represent the CCJ model fit. Reprinted from Fang et al. [63].

Dynamic Behavior

The study of the viscoelastic properties of ERFs under an applied electric field is especially crucial in real engineering applications, such as shock absorbers [64]. Dynamic loading is represented by oscillatory shear at sufficiently small strain (γ). In contrast to steady shear, the particle structures are only slightly deformed here without any destroying their internal structure. Viscoelastic properties are characterized by means of oscillatory dynamic experiment in the amplitude sweep and the frequency sweep modes [65, 66]. Dynamic behavior is then determined by complex shear modulus:

$$G^* = G' + G''$$ (6)

where G^* is complex shear modulus, G' is the storage modulus representing elastic part of the material, and G'' is the loss modulus representing viscous part of the material.

Firstly, for a description of dynamic behavior, the linear viscoelastic region has to be defined from amplitude sweeps under various external electric field strengths [64, 67]. It is region where both moduli are independent on γ and its location is shifted to a low (γ) side with the increase in electric field strengths (Fig. 4a). The chosen γ value from the linear viscoelastic region is further essential for frequency sweeps measurement. A typical curves of ER viscoelastic material under the frequency sweeps are shown in Fig. 4b. In off-state, the G'' is generally higher than G' indicating that ERF is still in the liquid state. However, after applying the electric field, G' becomes prevail over G'' due to the formation of the internal structures and the fluid exhibits solid-like behavior [68, 69].
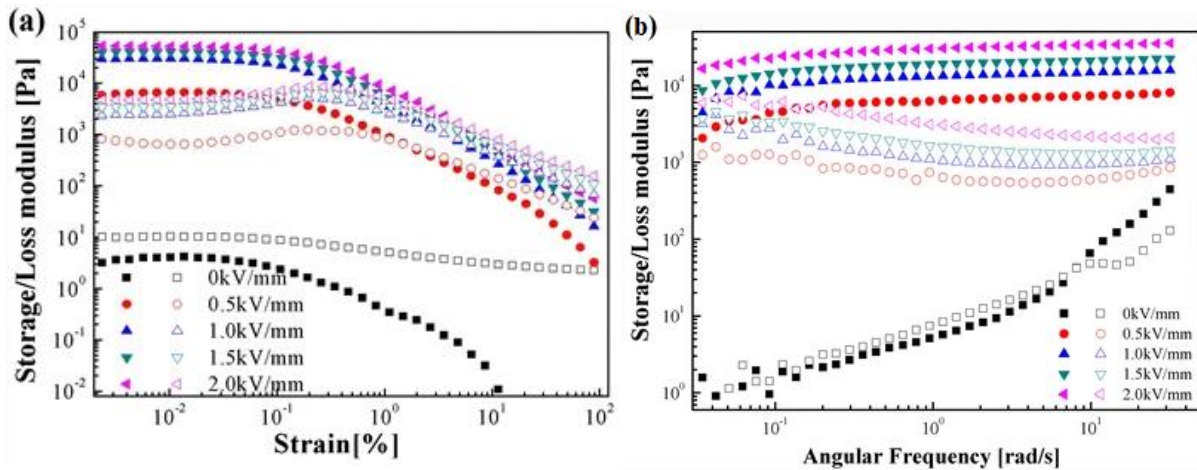

Fig. 4. Dependence of storage (solid symbols) and loss (open symbols) moduli on strain a) and on angular frequency b) for ERF containing microporous covalent triazine-based polymer particles under different electric field strengths. Reprinted from Dong et al. [68].

1.3.2 Dielectric Properties

Electrorheological fluids are two-component systems consisting of a non-conducting continuous liquid phase and electrically polarizable dispersed particles creating the internal chain-like structures owing to dipole-dipole interaction. It was concluded that particularly the interfacial Maxwell–Wagner polarization [70] located in the low-frequency range leads to the ER effect, and hence dielectric characterization of the ER suspensions is closely associated with the ER performance [38, 71]. Electrorheological effect is influenced by the dielectric relaxation time, the relative permittivity, the dielectric loss factor and the electrical conductivity of the particles [38].

Conductivity plays an immense role in ER performance as the formation of internal structures can only occur if the conductivity of the solid dispersed phase (σ_p) is higher than the conductivity of the liquid medium (σ_{lm}). Nevertheless, at too high value of σ_p, short circuit can be appeared due to high current density. The optimal conductivity of the material has to be adjusted, e.g., in the case of conducting polymers used as a dispersed phase, deprotonation or protonation process is applied [40, 72].

It has been demonstrated that the local electric field (E_L) between two particles is much higher than an overall electric field E. The value of E_L/E depends on $\varepsilon_p/\varepsilon_{lm}$, where ε_p and ε_{lm} are the relative permittivity of the dispersed particles and the insulating liquid medium. To achieve a high ER effect, a great mismatch between the relative permittivity of the particles and carrier medium is required. Further, the ER effect can be increased by introducing polar groups into the particles [73, 74].

Dielectric behavior of ERFs can be generally characterized using a Cole-Cole model [38]:

$$\varepsilon^*_{(\omega)} = \varepsilon'_{(\omega)} + i\varepsilon''_{(\omega)} = \varepsilon'_\infty + \frac{\varepsilon'_0 - \varepsilon'_\infty}{1 + (i\omega \cdot t_{rel})^{1-\alpha}} \tag{7}$$

where $\varepsilon^*_{(\omega)}$ is a complex permittivity, ε' and ε'' represent the relative permittivity and dielectric loss factor (the values lying in the range of $0.10 - 1$ kHz are crucial for the interfacial polarization), respectively [75]. The dielectric relaxation strength, $\Delta\varepsilon' = \varepsilon'_0 + \varepsilon'_\infty$, represents the interactions and polarization of the particles affected by the electric field. The symbols ε'_0 and ε'_∞ mean relative permittivity values at zero and infinitely large frequency, respectively [38, 76]. Further, parameter ω is angular frequency and t_{rel} is a relaxation time reflecting the polarization rate of the particles within suspension upon the application of an electric field. The exponent $1 - \alpha$ signifies the width of the distribution of the relaxation time which should lay in the frequency range $10^2 - 10^5$ Hz [38, 45]. However, the Cole-Cole model is limited and can be used only for a symmetric relaxation peak (Fig. 5).
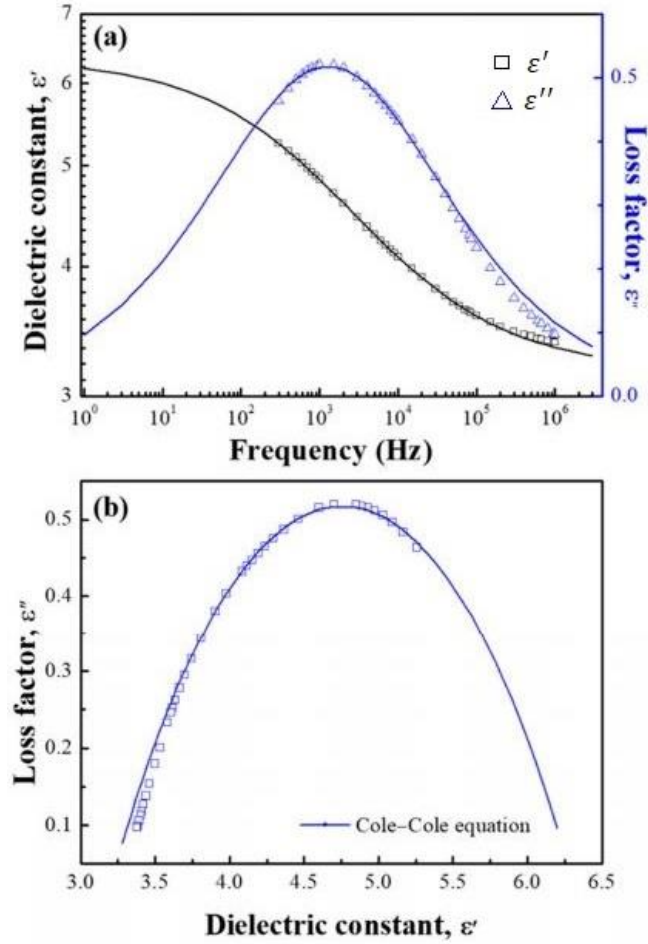
Fig. 5. Dependence of relative permittivity (black squares) and dielectric loss factor (blue triangles) on frequency (a) and dielectric loss factor (blue squares) on the relative permittivity (b) for the ERF based on poly(diphenylamine)/Fe₃O₄ (10 vol%). Solid lines represent the Cole-Cole model application. Reprinted from Dong et al. [41].

To obtain more accurate results from the dielectric spectroscopy measurements of the ERFs, Havriliak–Negami (H–N) model is applied (Fig. 6):

$$\varepsilon^*_{(\omega)} = \varepsilon'_\infty + \frac{(\varepsilon'_0 - \varepsilon'_\infty)}{(1 + (i\omega \cdot t_{\text{rel}})^\alpha)^\beta} \tag{8}$$

where ε'_0 is a relative permittivity at zero frequency, ε'_∞ is a relative permittivity at infinite frequency, ω is angular frequency ($2\pi f$), t_{rel} is a relaxation time, α and β are shape parameters both in the range of $0-1$ describing the asymmetry of the dielectric function [77, 78]. When $\alpha \neq 1$ and $\beta = 1$, Eq. 8 reduces to the Cole-Cole equation. The ERFs possessing higher dielectric relaxation strength and shorter relaxation time near the range of 1.6×10^{-3} to 1.6×10^{-6} s reach substantial ER effect [79, 80].
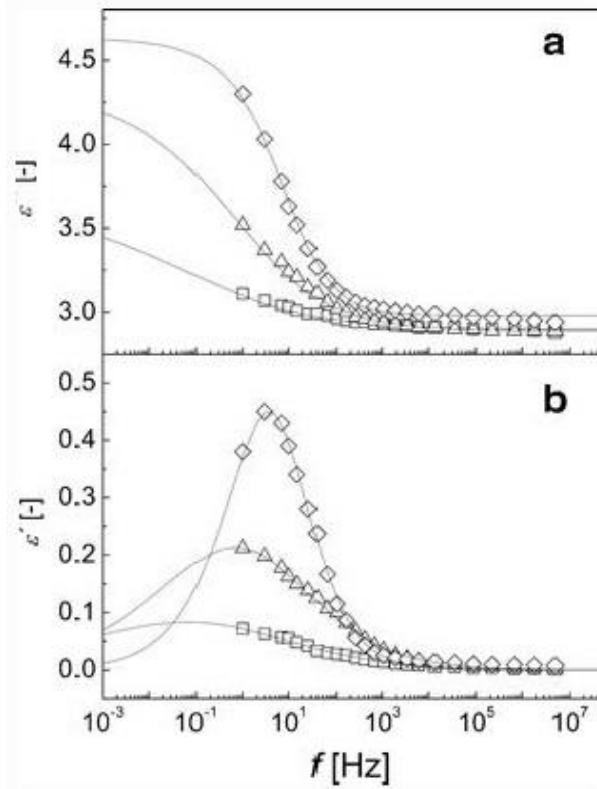
Fig. 6. Dependence of relative permittivity (a) and dielectric loss factor (b) on frequency for 10 vol% ERFs of aniline oligomers prepared in 0.1 M methanesulfonic acid (squares), 0.2 M methanesulfonic acid (up-pointing triangles), and 0.5 M methanesulfonic acid (diamonds). The solid lines represent the Havriliak–Negami model application. Reprinted from Mrlik et al. [79].

If the particles in the ERF are too conductive, electrode polarization can occur, and thus the typical interfacial polarization is difficult to recognize via H–N model. Hence, the model can be transformed into the form of a dielectric modulus (Fig. 7) [81]:

$$M^*_{HN}(\omega) = M_\infty + \frac{\Delta M}{(1 + (i\omega \cdot t_{rel})^\alpha)^\beta} \tag{9}$$

where t_{rel} is the relaxation time, ΔM is the dielectric relaxation strength, M_∞ is unrelaxed value of dielectric modulus, α and β are parameters represent the width and the skewness of the relaxation, respectively.
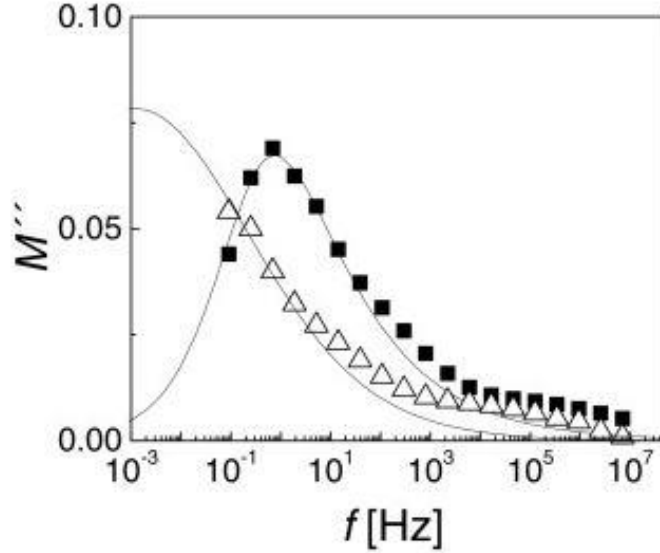
Fig. 7. Dependence of loss modulus on frequency for ERF based on molybdenum disulfide (squares) and tungsten disulfide (up-pointing triangles) particles coated with PANI dispersed in silicone oil. Reprinted from Mrlik et al. [81].

1.4 Factors Influencing the Electrorheological Effect

In addition to the type of dispersed electrically polarizable particles and the properties of liquid continuous phase, there are many other factors influencing the ER effect generated in ERFs. The most important are listed below.

1.4.1 External Electric Field Strength

The external electric field is essential for the formation of internal structures in ERFs. In the presence of an external electric field, τ_y of ERFs increases with increasing strength of this field applied. The yield stress is defined as the maximum stress which the ERF has to resist before starting to flow. Thus, a dependence of τ_y on an external electric field is presented by the power law model as follows [82]:

$$\tau_y = q \cdot E^\alpha \qquad (10)$$

where τ_y is the yield stress obtained by extrapolating the shear stress at zero shear rate, q is a rigidity of the whole system, E is the electric field strength and α is a slope of linear curve fitting the data.

Particles dispersed in the suspension can respond to electric field strength according to a polarization or a conduction model. In the case of the polarization model, the ER response ($\alpha = 2$) is affected by the electrostatic interactions between the dielectric particles leading to the formation of stiff internal chain-like structure in ERFs. On the other hand, if the ER response ($\alpha = 1.5$) is influenced by a fluid-

induced conductivity among particles, the conductivity model is expected (Fig. 8) [83, 84].
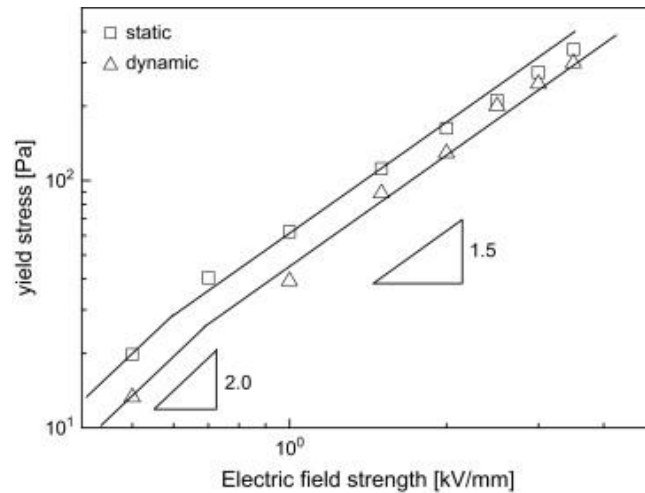

Fig. 8. Static and dynamic yield stresses as a function of electric field strength for 15 wt% dodecylbenzene-sulfonic acid-doped PANI based ERF. Reprinted from Kim et al. [84].

The value of α is generally in the range of 1.5 – 2, which has been proved by many researchers [85-87]; however, there are selected research papers demonstrating that the value of α could become smaller than 1.5 depending on the type of particles, their concentration, and morphology [88-90].

1.4.2 Interaction Forces within Electrorheological Fluids

Due to high external electric field, electrostatic forces acting on particles inside the fluid becomes immense. However, in addition to these forces, there are other forces in ERFs, such as hydrodynamic forces resulting from the viscous flow of the insulating liquid medium, Brownian forces due to thermal motion of liquid medium (discussed in the part 1.4.4), short-range repulsive forces, adhesive forces as a result of water bridge between the particles, and van der Waals interactions [91-94].

Brownian motion of the particles is observed much stronger in the case of less viscous carrier medium, smaller particles (less than 1 µm), and higher temperature. The relative importance of the hydrodynamic to thermal forces expresses the Peclet number (*Pe*) and the importance of the electric polarization to the thermal forces describes the parameter λ [91, 95]. In the ERFs, after application of electric field, at low shear rates, electric polarization forces dominate over hydrodynamic forces. On the contrary, the hydrodynamic forces start to dominate from a certain critical value of shear rates (Fig. 9) [84, 96].
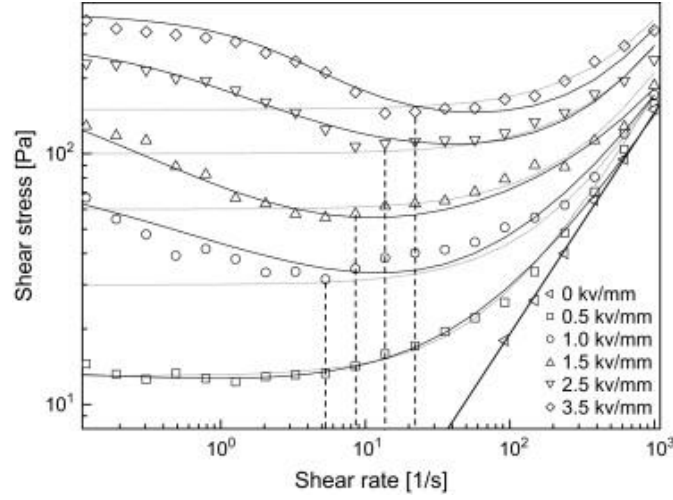
Fig. 9. Dependecies of shear stress on the shear rate for the ERF. The solid lines represent a fit according to CCJ model and the dotted lines represent the Bingham model. The dashed lines represent the critical shear rate. Reprinted from Kim et al. [84].

Hence, the Mason number was introduced as the ratio of the hydrodynamic to the polarization forces ($M_n = Pe/\lambda$) [91]. The dimensionless Mason number is defined as [68, 97, 98]:

$$M_n = \frac{\eta_c \dot{\gamma}}{2\varepsilon_0 \varepsilon_c (\beta E)^2} \tag{11}$$

where η_c is the viscosity of the continuous phase, $\dot{\gamma}$ is shear rate, ε_0 is the permittivity of the free space, ε_c is the relative permittivity of the continuous phase, E is the electric field strength and β is the relative polarizability of the particles [97]:

$$\beta = (\varepsilon_p - \varepsilon_c)/(\varepsilon_p + 2\varepsilon_c) \tag{12}$$

where ε_p and ε_c are the relative permittivities of the dispersed particles and the continuous phase.

Fig. 10 demonstrates the double-logarithmic plots of the relative viscosity, η/η_C (the ratio of the shear viscosity, η, to the viscosity of the continuous phase, η_C) vs. M_n. All data obtained at different electric field strengths and shear rates can be shown as single descending linear curve (a slope of -1.0) while its intersection with horizontal line corresponding to the high shear rate viscosity expresses the critical Mason number ($M_n{}^*$) [99]. The Mason number allows to collapse data onto the single common curve and it is useful for prediction of the ER behavior under different electric field for various particles. On the other hand,

M_n cannot be taken as a universal parameter for expressing the relative viscosity but as an approximate scaling [68, 95, 99].
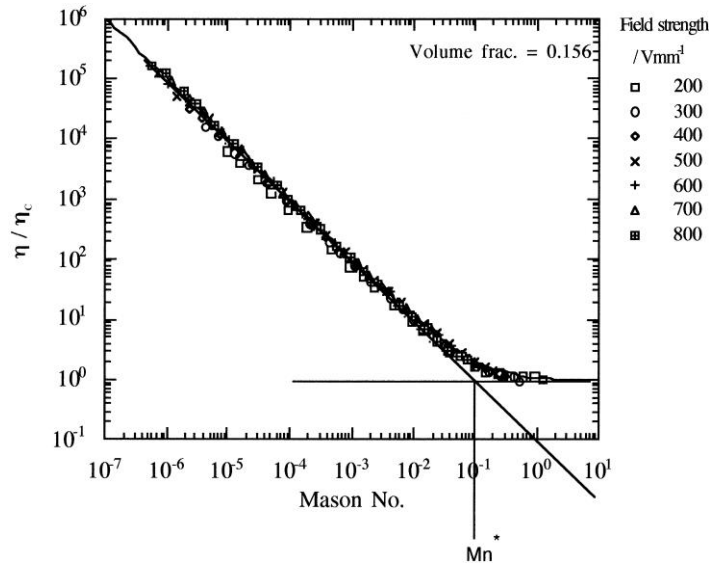

Fig. 10. The dependence of the relative viscosity on the Mason number for ERFs based on N-methylpyrrole at all applied field strengths. Reprinted from Goodwin et al. [99].

1.4.3   Particle Concentration, Size and Morphology

The electrorheological effect is closely related to the particle concentration, size and morphology. The optimal particle concentration for the highest achievable ER effect depends on the particle's response to an external electric field. A suitable volume fraction of dispersed particles usually reaches up to a maximum of 40 vol%, but it depends on particle size [18].

Huang and Wen et al. proposed a suspension consisting of barium titanyl oxalate nanoparticles dispersed in silicone oil, namely giant electrorheological (GER) fluids (Fig. 11), which reach the static τ_y of 130 kPa at the concentration of 30 vol% [100, 101]. In the case of nanoparticles, this concentration already appears to surpass the limit of the maximum usable for the smart fluids. Besides, Fig. 11 does not display the off-state viscosity, which can be considerably high, and thus, the system is not considered as a suspension.
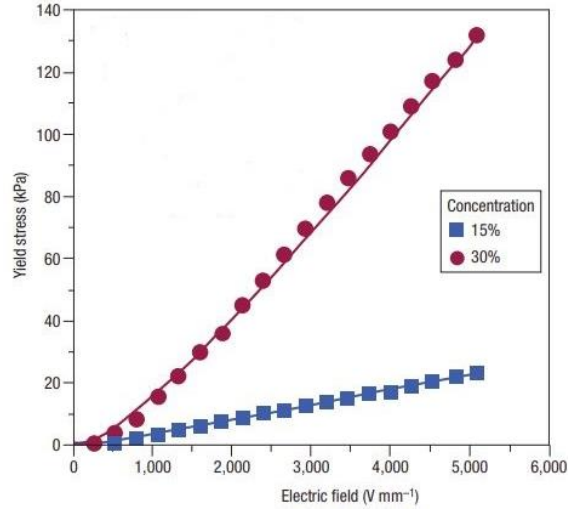
Fig. 11. Dependences of the static τ_y of GER fluids based on barium titanyl oxalate nanoparticles on applied electric field. Reprinted from Kim et al. [100].

The ER efficiency signifies the behavior change in the viscosity of the ERFs in the on-state and the off-state and can be expressed as in the following equation:

$$e = \frac{(\eta_E - \eta_0)}{\eta_0} \tag{13}$$

where η_E is viscosity in the presence of the external electric field (on-state) and η_0 is field-off viscosity [82].

It is evident that the ER efficiency increases with increasing concentration of particles (Fig. 12). Similarly, the field-off viscosity also increases with concentration (Fig. 13).
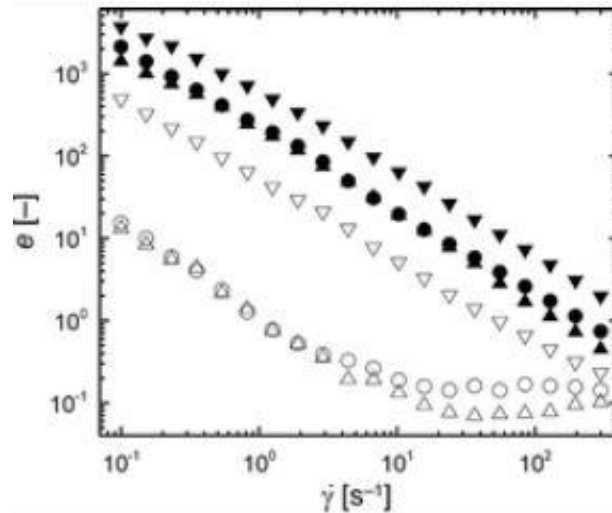

Fig. 12. The dependence of ER efficiency on the shear rate for ERFs based on anatase TiO2 globular nanoparticles (open) and rutile TiO2 rod-like (solid) microparticles. Concentrations of the particles are 5 wt% (triangles), 10 wt% (circles) and 15 wt% (inverted triangles). Reprinted from Sedlacik et al. [82].

20

Upon the application of an electric field, the viscosity of ERFs increases (Fig. 13) with the increasing volume fraction of dispersed particles; however, only up to a certain critical value due to interfacial polarization between the particles [83].
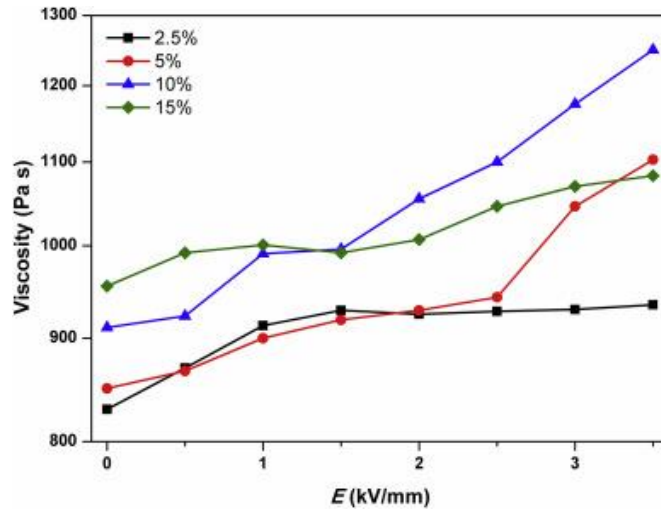

Fig. 13. Dependence of the viscosity of expanded perlite dispersed in silicone oil at various particle concentration (vol%) on the external electric field at shear rate of 1.0 s^{-1}. Reprinted from Cabuk et al. [83].

Morphology of the particles is also considered as a critical factor for sufficient ER effect. A number of experiments have shown that 1D and 2D particles (mostly represented by rods, fibers, and plates orienting their longer dimension in the direction of the electric field applied) contribute to a greater dipole-dipole interaction when compared to the spherical particles. Even at low particle concentration, the ER effect can be significantly influenced. Consequently, the permittivity, intrinsic viscosity, and dynamic modulus of the oriented internal structure in the ERFs increase with aspect ratio of dispersed particles [13, 102, 103]. It has been demonstrated that ERFs based on TiO_2 with a sole difference in their various morphology exhibited different ER behavior. The ERF based on rod-like TiO_2 particles possessed higher ER effect in comparison to the ERF based on globular TiO_2 [11]. In the case of plate-like particles, Tang et al. have proved that ERFs based on 2D PANI/TiO_2 nanosheets exhibit great enhancement of ER effect, very low field-off viscosity and improved yield stress compared to globular particles-based ERF due to interparticle friction [85].

Few research groups have dealt with an impact of particle size on ER performance. In electrorheology, the highest ER effect is usually observed for fluids containing dielectric nanoparticles possessing higher specific area which leads to higher surface polarization. The studies proved that ER effect is enhanced with decreasing the diameter of particle [100, 102, 104]. However, the size effect of particles on ER response has not been completely clarified yet as an evidence of the opposite trend has been published by McIntyre et al. [105]. The group

demonstrated that ER efficiency rose with an increase of the particle size because the yield stress representing the ER behavior is proportional to the size of particles. This theory was also confirmed by Lee et al. who analyzed silica nanoparticles with four different diameters. It was verified that the ER performance and yield stress was enhanced with the increase in particle size [106]. Consequently, it is always necessary to make a specific investigation for a certain material, size, and shape.

1.4.4 Temperature

From a practical application point of view, it is also necessary to consider the influence of temperature on the ER effect. Increased temperature leads to a change in the particle conductivity and relative permittivity resulting in the polarizability of ERFs being affected positively. On the other hand, particle thermal motion is directly influenced by increasing temperature. The Brownian motion significantly increases at high temperature and if is strong enough to overcome the particle creation, the ER effect is weakened [18]. It has been proved that ERFs based on hydrous materials exhibit decreasing ER effect with temperature because of the evaporation of water at elevated temperature. Therefore, these materials can only work in a narrow temperature range [107]. In contrast, ER effect of ERFs containing anhydrous materials could increase with temperature. For anhydrous materials, it would be possible to work in the range of higher temperatures, but the particle's conductivity is a limiting factor and it has to be controlled. In general, with increasing the temperature, the viscosity of the whole system decreases, and particles have better mobility in the suspensions, but the sedimentation stability would be reduced [18, 108]. Recently, Pan et al. have investigated (Fig. 14) the dynamic τ_y of the ER fluid based on copolymer synthesized of the monomers 1-allyl-3-methyl imidazolium chloride and N-isopropylacrylamide at different temperatures. The research group has found that the dynamic τ_y increased with increasing temperature. There was an inflection point above which the temperature dependence of the dynamic τ_y was more pronounced. This indicated that below a critical temperature, the polarization of the particles under an electric field was enhanced by increasing temperature [108].
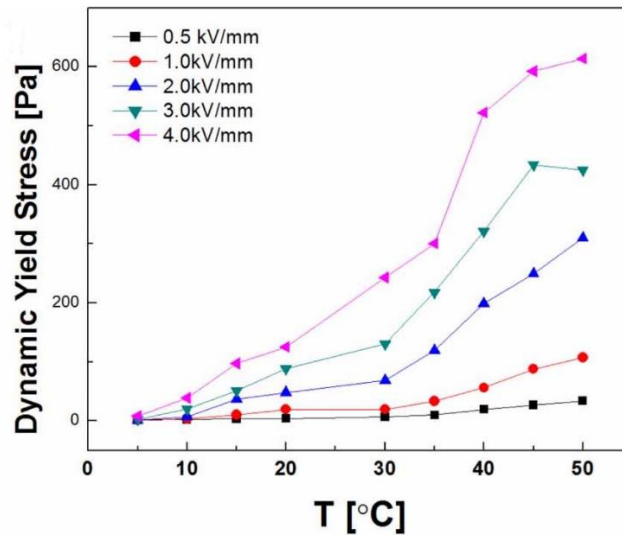
Fig. 14. Dependence of dynamic yield stresses on temperature for ERF based on copolymer 1-allyl-3-methyl imidazolium chloride and N-isopropylacrylamide under different electric field strengths. Reprinted from Pan et al. [108].

1.5 Applications of Electrorheological Fluids

The reversible transition from a liquid state to a solid-like state under an external electric field application makes the intelligent ERFs attractive in a wide range of engineering applications. Many ER devices have already been proposed in various engineering fields such as vibration suppression represented by ERFs-based damping devices [109, 110], brakes [111], medium in clutches [6, 112, 113], valves [114-116] etc. Some of them have been investigated for everyday life such as a rotational motion control of a washing machine with applied ER clutch or brake actuators [117], or three-dimensional tactile displays [118-120]. In addition, the ERFs can be also used in medicine as a human muscle stimulator [121] or as actuators for rehabilitation robotic devices [122-125].

1.6 Drawbacks of Electrorheological Fluids

One of the main issues of current ERFs is their low ER effect and poor sedimentation stability, which is discussed in detail below in a separate subchapter. Therefore, many ER devices have not been applied yet to real industrial applications.

The working temperature range is also an obstacle to a sufficient ER effect. If the working temperature exceeds 100 °C, the ER effect is substantially decreased [18]. For obtaining required ER behavior, the conductivity of the ERFs increases with increasing temperature and the external electric field of higher strengths cannot be applied due to the increment of the mobility of the charges [126]. Furthermore, for a high ER effect is desirable the τ_y as well as its thermo-oxidation stability for the consistency of the ER effect. The oxidizing carrier medium or particles can change the off-state viscosity (generally increases), τ_y

23

(generally decreases) or chemical composition and thus influencing negatively the ER effect of the whole system [127]. Last but not least, the high price of ERFs makes them very limited for commercialization.

Developed GER fluids achieve higher τ_y than conventional ERFs but their nanometer-sized particles are always connected with a high field-off viscosity, leading to a low ER efficiency. One of the approaches to achieve both low field-off viscosity and high τ_y values is a combination of large and small particles [14]. Moreover, at high concentrations, inorganic particles used for the GER fluids cause a significant abrasion of the system.

In the case of the ER devices, low field-off viscosity, low abrasiveness for long-term use, broad working temperature region, compatibility of dispersed dielectric particles to carrier liquid medium, and sedimentation stability are necessary for a functioning system [128].

1.6.1 Sedimentation Stability

Currently, most of the ERFs still display poor sedimentation stability due to the high density of the dispersed dielectric particles, which is one of their main obstacles for engineering applications [31]. Especially inorganic materials that possess a high density, could significantly increase their stability by coating the particles with a conductive polymer. Dong et al. have dealt with the synthesis of core-shell structured conducting polymer-coated nanoparticles. As can be seen in the Fig. 15, in the case of ERF based on conductive PANI coated onto the Fe_3O_4 particles, the sedimentation stability has been improved. It has been investigated that except density, morphology, size, surface characteristics, and particles concentration also affect the sedimentation stability of the ERFs. Higher particle concentration enhances the sedimentation stability since particle-particle interactions and particle-liquid ones are increased [129]. In addition, it has been demonstrated that rod-like particles exhibit better sedimentation stability when compared to globular particles owing to the limited rotation motion in the liquid medium [130].
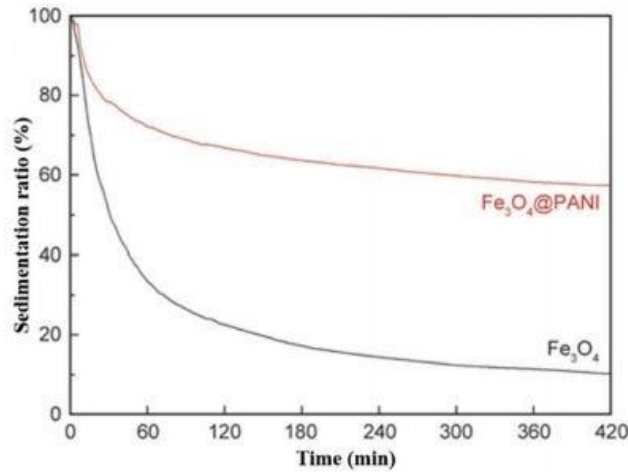
Fig. 15. Sedimentation stability of the ERFs containing Fe₃O₄ and Fe₃O₄/PANI particles at the concentration of 20 wt%. Reprinted from Dong et al. [129].

The sedimentation stability of the ERFs is mostly evaluated by using a visual observation [31, 131], an optical analyzer (Turbiscan) [57, 132], or using the tensiometer [133].

The most common way for the sedimentation stability evaluation is simple naked-eye observation. Graduated cylinder is used for recording a phase separation height between the particle-rich phase and the relatively clear liquid phase depending on the time. The sedimentation ratio is then obtained as a height of the particle-rich phase relative to the total system height [134, 135].

The optical analyzer, e.g. Turbiscan, with two synchronous optical sensors measures the backscattering and transmission of monochromatic light (usually at wavelength of 880 nm) in the measured system. The ERF is placed into flat-bottomed cylindrical glass tube and to acquire data, the detection head periodically scans a sample from bottom [57, 136]. Turbiscan allows fast detection of the sedimentation in the order of one hour or less. It can also detect agglomeration or clarification during the aging of ERFs. However; in many applications, long-term stability reaching a few days is necessary, and for this reason, simple observation method seems to be sufficient for the investigation of sedimentation stability [137].

The third method for evaluation of sedimentation stability of ERFs can use a tensiometer, which works on the principle of measuring a probe, which is in contact with the surface of dispersed ERF and subsequently controllably immersed into the fluid. This probe then records the weight of the falling particles as a function of time. Nonetheless, this method has so far been used more for magnetorheological fluids but the most probably it can also be used in the case of ERFs [133, 138].

25

1.7 State of the Art

Currently, researchers are still working on improvements in the ERFs applied research and to minimize existing shortcomings as much as possible. New techniques as well as development of materials have been investigated.

Although titanium dioxide has belonged to a widely studied group of materials [130, 139, 140] in the field of electrorheology for a few years, the authors [141] decided to prepare novel core–shell material where silicon oxide was used as the shell material presented on titanium dioxide core. Nonetheless, many previous studies have been published mostly utilizing silicon oxide as the core and titanium dioxide as the shell due to its high relative permittivity. Hollow peanut-like anisotropic core–shell nanoparticles TiO_2/SiO_2 were successfully synthesized. The prepared ERFs exhibited excellent sedimentation stability, unique morphology and τ_y reaching approximately 200 Pa (10 wt%) at the electric field strength of $3\,kV\cdot mm^{-1}$.

Further study [142] demonstrated the fabrication of a novel architecture of high performance dielectric particles is worthy of attention not only for the potential ERFs applications but also for electromagnetic wave attenuation. Zhang et al. synthesized PANI nanoneedles on the exfoliated MoS_2 nanosheet matrix by means of an in-situ oxidation polymerization. The dielectric properties, tunable electric conductivity, and ER performance were enhanced $-\tau_y \approx 180\,Pa$ (15 wt%) at $3\,kV\cdot mm^{-1}$. Electrorheological efficiency was increased exceedingly in comparison to ERFs based on bare MoS_2.

In recent years, new ER material based on poly(ionic liquid) has been introduced. The research group of Zhang et al. [143] has synthesized the imidazolium-based poly(ionic liquid) with tetrafluoroborate as anion. The prepared microspherical particles was mixed with silicone oil at the concentration of 15 wt%. Upon the application of the electric field strength of $3\,kV\cdot mm^{-1}$, dynamic τ_y obtained from the CCJ model achieved about 400 Pa. The power law model implied the low conductivity of the particles, polarization model was described.

Research on ER systems is furthermore currently focused on improving applications, such as supercapacitors, which can only be used for short-term energy storage due to their self-discharge problem. Therefore, in this study [144], a new approach was introduced to reduce the self-discharge of supercapacitor based on the ER effect and improve their applications for environmental energy harvesting and storage. Liquid crystal molecules were used as ER material, in which the viscosity of the electrolyte significantly increased after the electric field was applied, preventing the diffusion of ions in the electrode. The use of ER liquid crystal enhanced the charging efficiency from environmental energy harvesting and extended the power charging for small devices.

The last study from ERFs [145], describes a unique design of ER bending-type actuators with an alternating pressure source for small-scale systems, including

their actuation and sensing mechanisms integrated within the robot body. A research team presented 1.6 mm long ER bending actuators with high aspect ratio and three-dimensional structures, which were prepared by a newly polydimethylsiloxane micromolding process. The ER actuator is composed of a bending part, ER microvalves, and a pressure transmitter. The nematic liquid crystal is used as a working ERF in the ER microvalves.

2. MOTIVATION AND AIMS OF THE DOCTORAL STUDY

2.1 Motivation

The ERFs represent a unique group of intelligent materials capable of changing their rheological properties reversibly and rapidly after application of an external electric field. These materials have been exploited in many industrial applications but still suffer from some issues, which prevent their full commercialization. Thus, to achieve better ER performance, researching new materials and eliminating above-described problems of current ERFs is essential.

2.2 Aims of Doctoral Study

The main attention of this study is focused on the preparation of new one-dimensional and two-dimensional ER materials, which show certain benefits in current electrorheology compared with the spherical particles. Especially rod-like particles having a high aspect ratio, which contributes to enhanced ER effect. Furthermore, a simple synthesis of rod-like particles and a novel modification approach is introduced. Investigation of prepared ERFs is performed by rheological measurements both in the absence and in the presence of an external electric field and dielectric spectra analysis. What is further expected, sedimentation stability of ERFs based on used dielectric particles should be considerably improved.

3. EXPERIMENTAL PART

This thesis deals with the investigation of suitable ER particles to increase the ER effect in comparison with ongoing research by other authors. The most crucial results from the papers published so far are summarized below.

Firstly, it was decided to synthesize our own ER materials, which could demonstrate the preferable ER effects. The results are introduced in **Paper I – Electrorheological behavior of iron (II) oxalate micro-rods**. The particles based on iron(II) oxalate ($FeC_2O_4 \cdot 2H_2O$) possessing required rod-like morphology with relatively high aspect ratio were successfully synthesized via a co-precipitation method [146]. The major advantage of this technique is its simplicity, cost-effectiveness, and the possibility of large-scale production. The synthesis was accomplished by mixing sulphate heptahydrate, and oxalic acid dihydrate in an equivalent amount. Under controlled synthesis conditions, it is possible to prepare the morphology of the desired shapes and sizes with high purity. Scanning electron microscopy was used to observe the morphology and size of the prepared particles.

Subsequently, ERFs were prepared at three concentrations, namely 1, 5, and 10 vol%. As it can be clearly seen in Fig. 16, the values of shear stress increased with increasing concentration of the particles and electric field strength. The ERF consisting of 10 vol% of $FeC_2O_4 \cdot 2H_2O$ particles achieved substantially higher shear stress values, approximately more than 1.5 orders of magnitude when compared to particles at lower concentrations. This ERF possessed a τ_y of about 80 Pa in the presence of the electric field with the strength of 1.5 kV·mm^{-1}. A typical trend of nearly Newtonian behavior was observed for all investigated ERFs in the absence of an electric field as well as in the so called on-off experiment, in which an electric field is altering between zero and a specific value of external electric field applied with time, confirming the reversible character of ERFs. Electrorheological performance of prepared suspensions is thus comparable with conventional materials synthesized in the multi-step reactions [69, 140]. Cho-Choi-Jhon model defined in Eq. 5 was used for further evaluation of measured data.
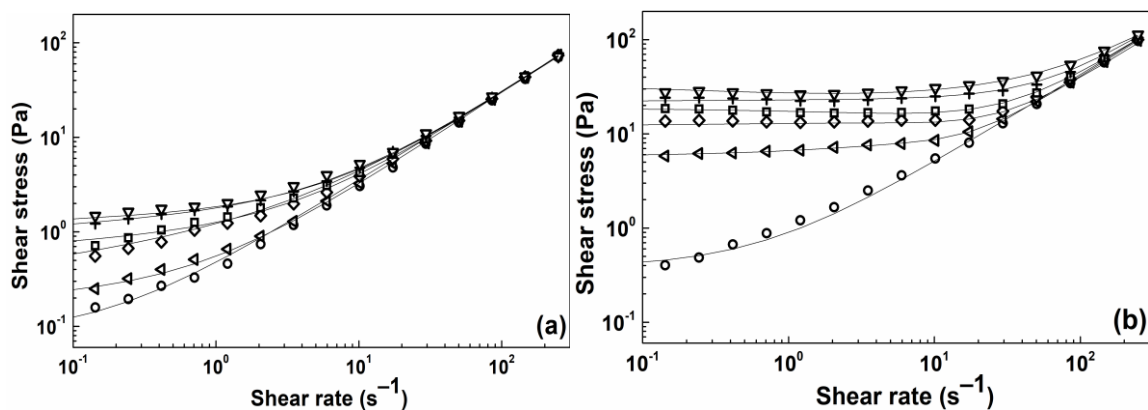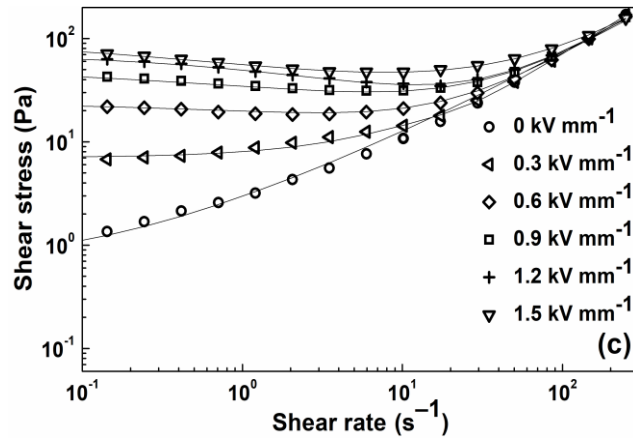
Fig. 16. Dependences of the shear stress on the shear rate for the ERFs based on the iron(II) oxalate particles at concentrations of 1 vol% (a), 5 vol% (b), and 10 vol% (c) in the absence of an electric field (circles) and in the presence of an electric field strengths of 0.3 kV·mm^{-1} (left triangles), 0.6 kV·mm^{-1} (diamonds), 0.9 kV·mm^{-1} (squares), 1.2 kV·mm^{-1} (crosses), and 1.5 kV·mm^{-1} (down triangles). The solid lines refer to the CCJ model fit. Reprinted from Kutalkova et al. [146].

The ER efficiency is an important factor describing the difference in the field-off viscosity and on-state viscosity. In the case of ERFs containing iron(II) oxalate particles, the highest ER efficiency was observed at the concentration 5 vol% and the electric field strength of 1.5 kV mm^{-1} (Fig. 17). It is evident that further increase in particles concentration does not positively influence ER efficiency because field-off viscosity is also raised.
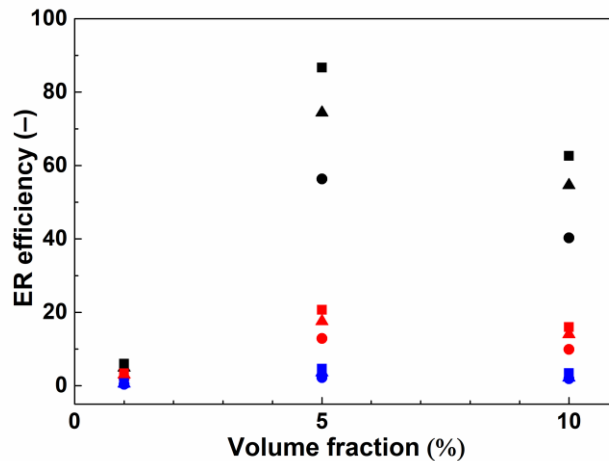
Fig. 17. Dependences of the ER efficiency on the particle volume fraction at the shear rates of 0.1 s^{-1} (black), 1 s^{-1} (red) and 10 s^{-1} (blue) in the presence of an electric field strengths of 0.9 kV·mm^{-1} (circles), 1.2 kV·mm^{-1} (up triangles) and 1.5 kV·mm^{-1} (squares). Reprinted from Kutalkova et al. [146].

30

Sedimentation stability of prepared ERF containing 5 vol% of iron(II) oxalate particles is shown in Fig. 18. Due to rod-like particle morphology, it is obvious that ERF remained stable for a long time. The sedimentation ratio achieved about 0.86 after about 42 hours which is a considerable improvement in comparison to published conventional ERFs [147, 148].
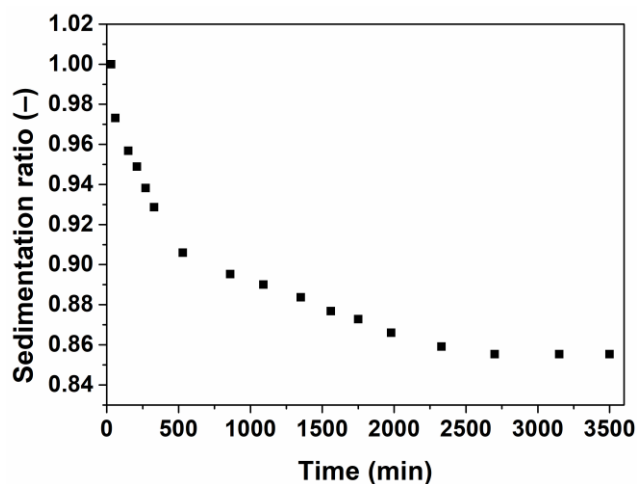

Fig. 18. The sedimentation stability of the ERF based on the iron(II) oxalate particles at the concentration of 5 vol%. Reprinted from Kutalkova et al. [146].

Iron(II) oxalate particles appears to be a suitable material for practical ER applications. Consequently, our effort was to expand this existing research by other iron(II) oxalate morphologies depending on the reaction conditions of synthesis. The results are summarized in **Paper II – Influence of synthesis conditions on electrorheological performance of iron (II) oxalate.** Fifteen various iron(II) oxalate samples were prepared by the co-precipitation method differing in synthesis conditions [149]. Subsequently, the effect of synthesis conditions on particles morphology was evaluated using a scanning electron microscopy. Based on this analysis, four samples were selected for testing their ER behavior. Table 1 shows the main synthesis parameters influencing the morphology of particles and calculated particles aspect ratio. The faster stirring speed proved to lead to faster growth of crystalline particles and more robust rod-like morphology, as shown in Fig. 19b and Fig. 20b. Furthermore, it can be concluded from Table 1 that the aspect ratio (*L/D*) did not change with the drip rate and stirring speed of the reaction mixture. In contrast, the length (*L*) was considerably different since longer particles were obtained at higher stirring speed of the reaction mixture regardless of the oxalic acid dehydrate's drip rate.

Table 1. Synthesis conditions for iron(II) oxalate particles investigated in and their dimensional characteristics. Reprinted from Kutalkova et al. [149].

Synthesis conditions			Code	L	D	L/D
Drip rate	Stirring speed	Stirring				
[mL/h]	[rpm]	[hrs]		[µm]	[µm]	[–]
2.30	100	2	OX1	0.90	0.17	5.29
2.30	500	2	OX2	2.20	0.33	6.67
1.16	100	2	OX3	1.24	0.16	7.75
1.16	500	2	OX4	2.24	0.43	5.21
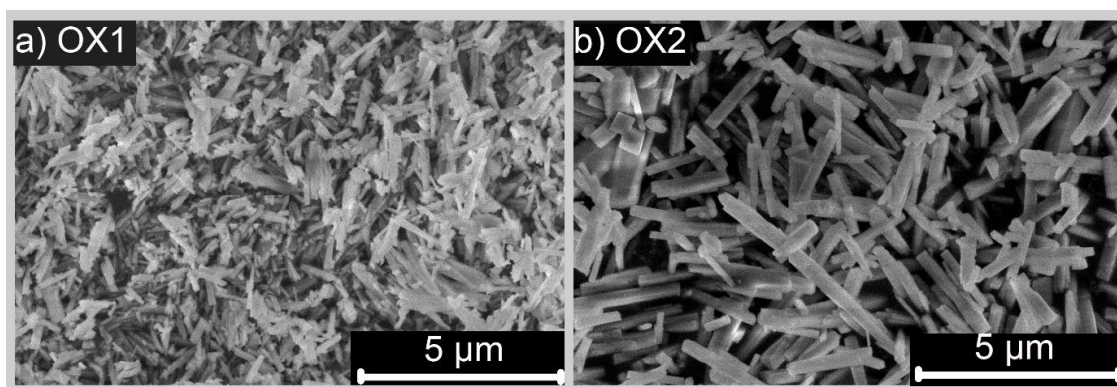
Fig. 19. SEM images of OX1 (a) and OX2 (b) particles. Reprinted from Kutalkova et al. [149].
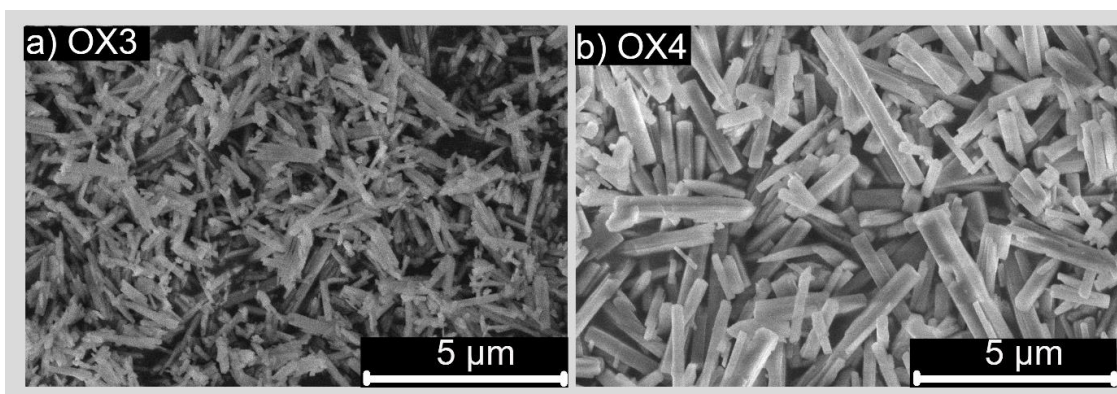
Fig. 20. SEM images of OX3 (a) and OX4 (b) particles. Reprinted from Kutalkova et al. [149].

Electrorheological fluids with 5 vol% concentration of $FeC_2O_4 \cdot 2H_2O$ particles were prepared by dispersion in silicone oil. In the presence of the electric field strength of 1.5 $kV \cdot mm^{-1}$ (Fig. 21), sample OX3 exhibited the highest ER effect and also ER efficiency, which is not shown here for brevity. This can be attributed to its high L/D, which plays a substantial role in ER performance as a result of the creation of stiffer internal chain-like structures. The remaining three samples demonstrate a similar ER effect to each other (Fig. 21).
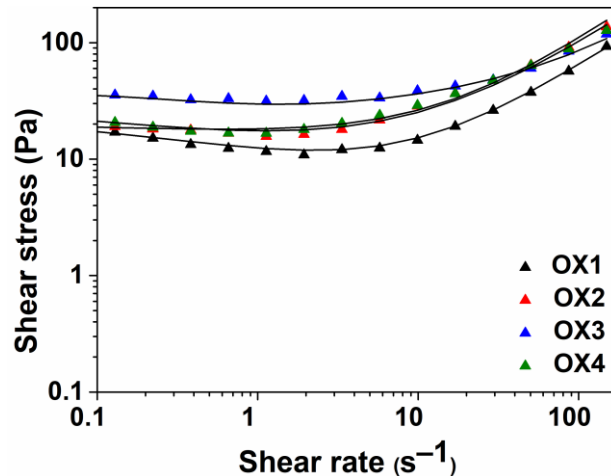
Fig. 21. Dependences of shear stress on shear rate for ERFs based on iron oxalate(II) particles synthesized under various conditions dispersed (5 vol%) in silicone oil in the presence of the electric field strength of 1.5 kV·mm−1. Solid lines represent the CCJ model fit. Reprinted from Kutalkova et al. [149].

Sedimentation stability of prepared ERFs was evaluated by visual observation of phase separation height in time (Fig. 22). The highest sedimentation ratio (≈ 0.9) after even 10 hrs was unequivocally observed for the sample OX3, apparently due to its morphology. From the application point of view, this is considered as beneficial result, especially at such low particle concentration.
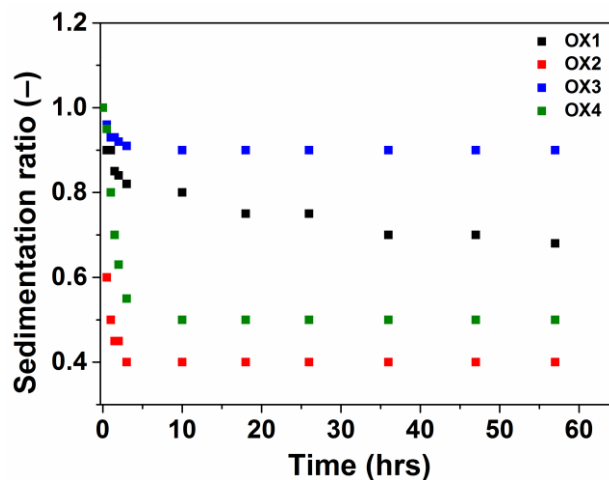

Fig. 22. The sedimentation stability of the ERFs based on the iron(II) oxalate particles (5 vol%) synthesized under various synthesis conditions dispersed in a silicone oil. Reprinted from Kutalkova et al. [149].

As aforementioned several times, poor sedimentation stability of ERFs is an issue that hinders their wider utilization. In the study **Paper III – On the enhanced sedimentation stability and electrorheological performance of intelligent fluids based on sepiolite particles** we decided to employ clay material based on sepiolite particles to investigate the possibility of improving the ERFs long-term sedimentation stability [150]. Commercial sepiolite particles were used for the preparation of ERFs. Scanning electron microscopy confirmed needle-like morphology of these particles with the high L/D of about 40.

Electrorheological properties of prepared silicone oil-fluids (concentration of sepiolite particles 5, 10 and 15 wt%) were analyzed in modes of controlled shear rate and controlled shear stress. Even in the absence of an electric field, ERFs exhibited a level of pseudoplastic behavior due to their formed gel-like structures with internal static τ_y. Even though Newtonian behaviour is more favourable, formation of a gel-like structure can hinder sedimentation in the off-state. From a steady shear testing in controlled shear stress mode, static τ_y values were determined as increasing substantially in line with concentration of sepiolite particles (Table 2).

Table 2. Static yield stress of ERFs containing 5 wt%, 10 wt% and 15 wt% of sepiolite particles in off and on-state. Reprinted from Kutalkova et al. [150].

Electric field strengths, E (kV·mm^{-1})	Static yield stress (Pa)		
	Concentration of the sepiolite particles		
	5 wt%	10 wt%	15 wt%
0	≈1.0	≈1.2	≈37.0
1	≈2.3	≈4.3	≈66.0
2	≈7.8	≈10.0	≈66.6
3	≈11.2	≈21.5	≈70.0

Viscoelastic moduli described a transition from a liquid-like to a solid-like state initiated by applying an external electric field (Fig. 23b). Electrorheological fluid containing 5 wt% of sepiolite particles exhibited higher G'' values compared to G' in the absence of an external electric field, which indicated that the ERF behaves as a liquid-like material (Fig. 23a). On the other side, fluids with concentration of 10 wt% and 15 wt% of sepiolite particles possessed higher G' than G'' values when no field was applied, which means that the internal stiff gel-like structure were confirmed even in the off-state. In the on-state, G' dominated over G'' for all the investigated ERFs, and additionally, both viscoelastic moduli increased of

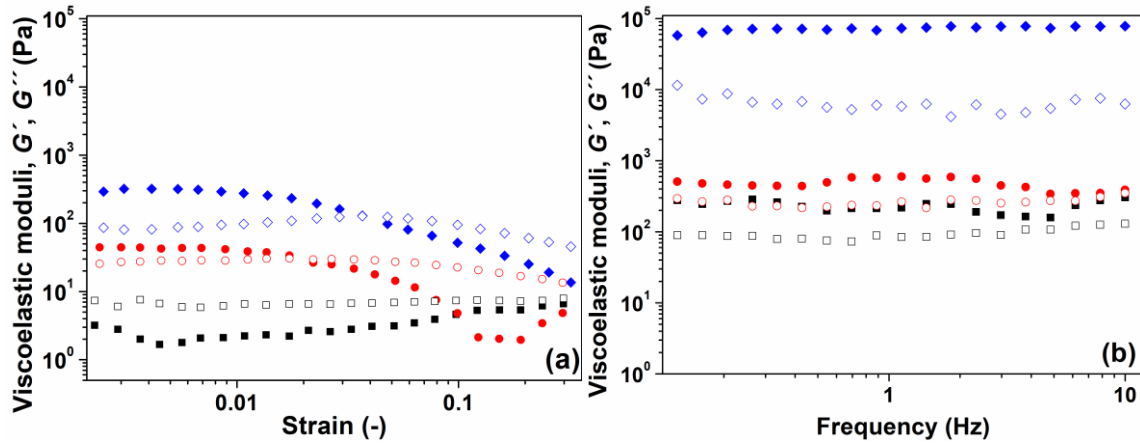about two orders of magnitude in comparison with ER performance in the off-state.

Fig. 23. Dependence of storage modulus (solid symbols) and loss modulus (open symbols) on strain at 0 kV·mm⁻¹ (a) and on frequency at 3 kV·mm⁻¹ (b) for the ERFs based on sepiolite particles at concentrations of 5 wt% (squares), 10 wt% (circles) and 15 wt% (diamonds). Reprinted from Kutalkova et al. [150].

As expected, increasing the level of sepiolite particles concentration brought extraordinary sedimentation stability, especially for the sample consisted of 15 wt% of sepiolite particles with sedimentation ratio of 1 after 200 hrs (Fig. 24). Based on these results, it was deduced that the sepiolite-based ERFs have to possess a certain level of internal static τ_y without applying an external electric field. However, this ERF achieved insignificant ER effect, and the highest ER efficiency was found for the ERF with the concentration of 5 wt% of sepiolite as a result of its lower field-off viscosity. The question has arisen regarding utilizing such excellent sepiolite particle stability and simultaneously reaching a high ER effect. In this case, the modified graphene oxide (GO) offers future research a suitable candidate for subsequent possible addition to the sepiolite-based ERF.
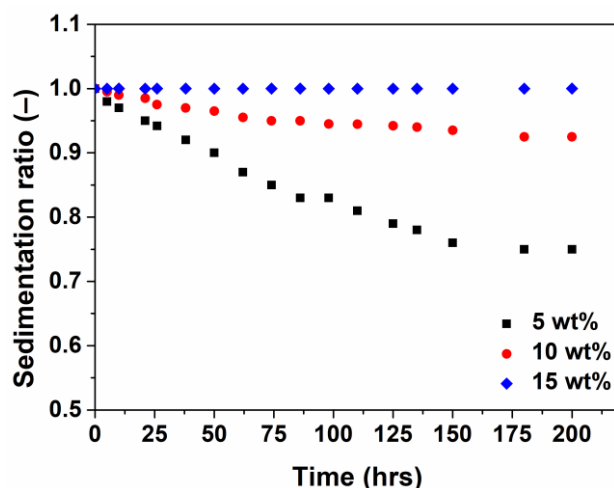
Fig. 24. The sedimentation stability of the ERFs containing 5 wt% (squares), 10 wt% (circles) and 15 wt% (diamonds) of sepiolite particles in silicone oil. Reprinted from Kutalkova et al. [150].

One of the most promising materials in electrorheology is graphene oxide which was non-covalently modified in two steps by various polymers [151]. Consequently, a new approach of GO modification has been introduced in the **Paper IV – Enhanced and Tunable Electrorheological capability using surface initiated atom transfer radical polymerization modification with simultaneous reduction of the graphene oxide by silyl-based polymer grafting**. This study was focused on the modification of the GO particles by surface-initiated atom transfer radical polymerization (SI-ATRP) of 2-(trimethylsilyloxy)ethyl methacrylate (HEMATMS) [135]. Graphene oxide sheets were prepared by a modified Hummers method [152] – graphite as a precursor of GO, sulfuric acid sodium nitrate, potassium permanganate, and hydrogen peroxide were used as oxidation agents. In order to prevent sedimentation of GO particles and to improve weak GO affinity to carrier liquid, GO particles were modified with HEMATMS via SI-ATRP. To obtain covalent bonds on the surface of GO, the esterification reaction between the –OH groups of GO and double-functional α-bromoisobutyryl bromide in the presence of triethylamine was performed. The final SI-ATRP grafting method is presented in Fig. 25.
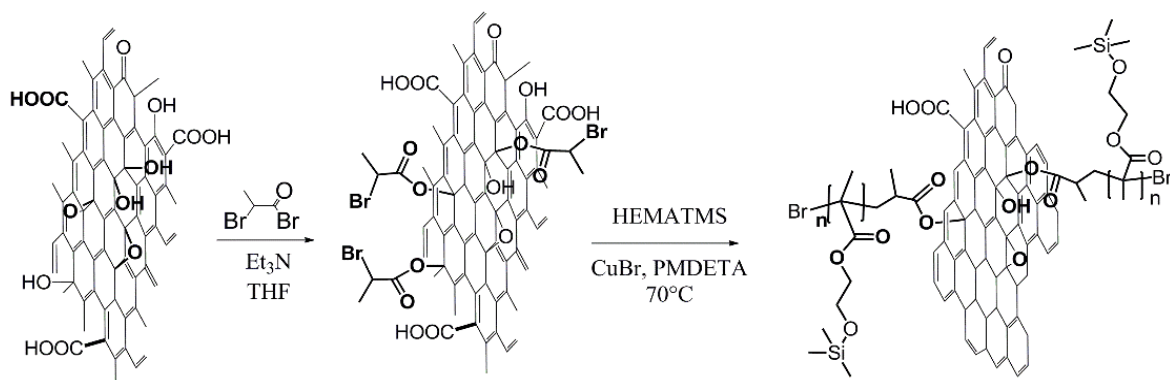
Fig. 25. Schematic illustration of the attachment of the ATRP initiator and grafting of the PHEMATMS from the GO surface with simultaneous partial reduction of the GO surface. Reprinted from Kutalkova et al. [135].

Two different chain-lengths (marked as GO-PHEMATMS_1 and GO-PHEMATMS_2, respectively) were prepared by the various molar ratio of reactants. Obtained molar masses were 12 600 g·mol^{-1} and 20 400 g·mol^{-1} with the polydispersity indexes of 1.19 and 1.13 for GO-PHEMATMS_1 and GO-PHEMATMS_2, respectively.

The successful grafting was confirmed using a transmission electron microscopy and a Fourier-transform infrared spectroscopy. Fig. 26 shows a well covered GO sheet-like structure with a polymer compact layer onto its surface.
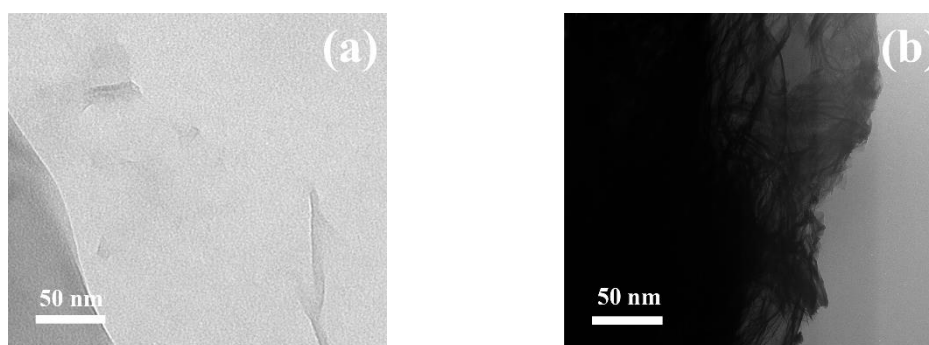
Fig. 26. Transmission electron microscopy images of unmodified GO (a) and modified GO-PHEMATMS_2 particles (b). Reprinted from Kutalkova et al. [135].

Electrorheological fluids containing GO-PHEMATMS_1 and GO-PHEMATMS_2 were prepared at a concentration of 5 wt% in silicone oil. As can be seen in Fig. 27, in the absence of an electric field, original GO particles exhibited typical linear Newtonian behavior. However, modified GO-PHEMATMS_2 particles showed small divergence from the flow behavior as a result of improved affinity between the dispersed particles and liquid medium, which consequently led to the enhanced sedimentation stability. The decrease in surface free energy of GO particles after their grafting resulted in better GO–silicone oil interactions. In the presence of an external electric field, ER effect increased almost up to 200 Pa at 2.5 kV·mm^{-1} for modified GO- PHEMATMS_2.

All three samples followed the conduction model as dominant factor for the ER performance.
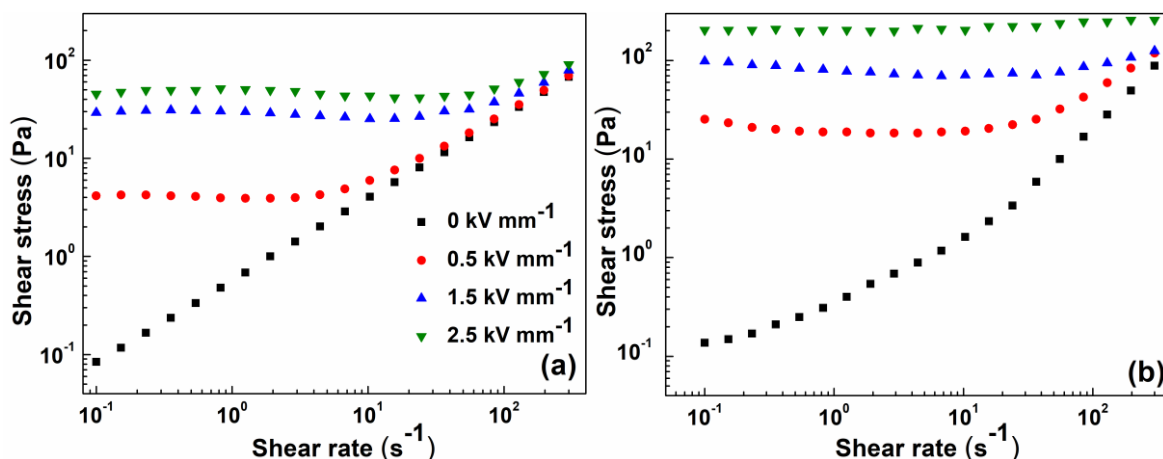

Fig. 27. Dependences of the shear stress on the shear rate for 5 wt% ERFs based on original GO (a), GO-PHEMATMS_2 particles (b) in silicone oil. Reprinted from Kutalkova et al. [135].

The dielectric measurement of these ERFs was also investigated, and dielectric parameters were obtained using a modified form of H–N model according to Eq. 9 (Fig. 28). Dielectric relaxation strength was increased with the polymer's molar mass and showed higher values for modified samples than for original GO. Relaxation time was shorten with the molar mass of the polymer suggesting a faster ER response of the samples on the external electric field applied.nm
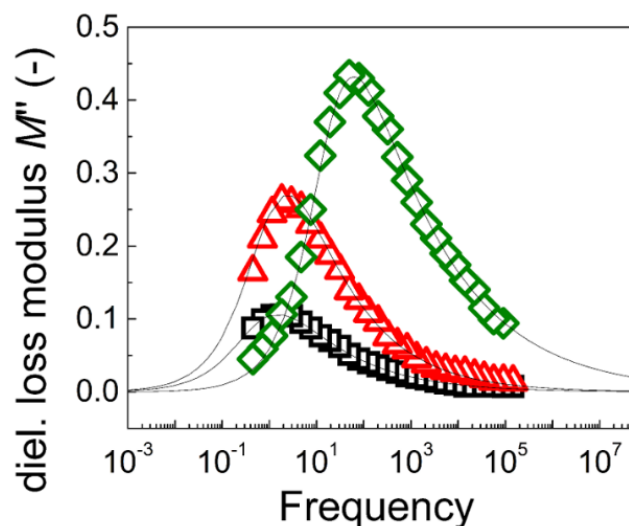
Fig. 28. Dependence of dielectric loss modulus on frequency for 5 wt% ERFs based on original GO (squares), GO-PHEMATMS_1 (up triangles), and GO-PHEMATMS_2 (diamonds) particles in silicone oil. Reprinted from Kutalkova et al. [135].

Sedimentation stability was also here proved by visual observation of investigated ERFs at a concentration of 5 wt% (Fig. 29). Improved compatibility of the grafted GO by PHEMATMS with silicone oil resulted in extremely enhanced stability against sedimentation in comparison to pure GO particles. The sample with longer polymer chains (GO-PHEMATMS_2) exhibited the higher sedimentation ratio as a result of the more lyophilic character of grafted particles.
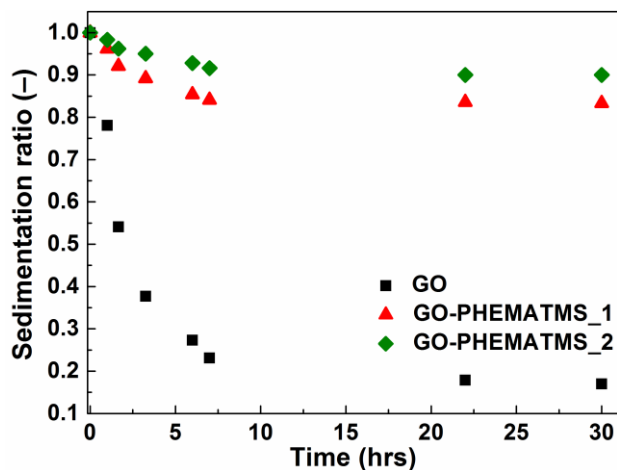

Fig. 29. The sedimentation stability of the ERFs containing 5 wt% of GO particles (squares), GO-PHEMATMS_1 (up triangles), and GO-PHEMATMS_2 (diamonds) in silicone oil. Reprinted from Kutalkova et al. [135].

4. CONTRIBUTION TO THE SCIENCE

This doctoral study's main aim was to find new materials for the preparation of intelligent ERFs, which would provide a solution to the current limiting issues, such as the weak effectiveness and the poor sedimentation stability of the ERFs, and consequently, to widen the options of their implementation in certain industrial applications.

Electrorheological materials based on iron(II) oxalate and modified graphene oxide were prepared via a simple co-precipitation reaction and controllably grafted using SI-ATRP, respectively. Besides, the ERF containing natural clay material was used and exhibited the excellent stability and availableness. A significant influence of the particle aspect ratio on ER effect and sedimentation stability has been demonstrated. The obtained results brought sufficient ER effects and the long-term stability enhancement of prepared ERFs in comparison with conventional, which can be beneficial to the scientific community as well as in specific industrial applications.

The achieved outputs were presented at international conferences and summarized in four papers, which were already published in journals indexed in Web of Science database. In addition, based on achieved results, it is expected that this research will be expanded in the near future and will be given the opportunity to get even closer to the requirements of real-life applications.

REFERENCES

[1] BENETTI, E. M.; CHUNG, H. J.; VANCSO, G. J. Ph responsive polymeric brush nanostructures: Preparation and characterization by scanning probe oxidation and surface initiated polymerization. *Macromol Rapid Commun.* **2009**, vol. 30, no. 6, pp. 411-417.

[2] JONAS, A. M.; GLINEL, K.; OREN, R.; NYSTEN, B.; HUCK, W. T. S. Thermo-responsive polymer brushes with tunable collapse temperatures in the physiological range. *Macromolecules.* **2007**, vol. 40, no. 13, pp. 4403-4405.

[3] WALSH, Z.; SCARMAGNANI, S.; BENITO-LOPEZ, F.; ABELE, S.; NIE, F. Q.; SLATER, C.; et al. Photochromic spiropyran monolithic polymers: Molecular photo-controllable electroosmotic pumps for micro-fluidic devices. *Sens Actuator B-Chem.* **2010**, vol. 148, no. 2, pp. 569-576.

[4] DE VICENTE, J.; SEGOVIA-GUTIERREZ, J. P.; ANDABLO-REYES, E.; VEREDA, F.; HIDALGO-ALVAREZ, R. Dynamic rheology of sphere- and rod-based magnetorheological fluids. *J Chem Phys.* **2009**, vol. 131, no. 19, 194902.

[5] WINSLOW, W. M. Induced fibration of suspensions. *J Appl Phys.* **1949**, vol. 20, no. 12, pp. 1137-1140.

[6] MADEJA, J.; KESY, Z.; KESY, A. Application of electrorheological fluid in a hydrodynamic clutch. *Smart Mater Struct.* **2011**, vol. 20, no. 10, 105005.

[7] LEE, S.; LEE, J.; HWANG, S. H.; YUN, J.; JANG, J. Enhanced electroresponsive performance of double-shell SiO2/TiO2 hollow nanoparticles. *ACS Nano.* **2015**, vol. 9, no. 5, pp. 4939-4949.

[8] KIM, Y. K.; LEE, Y.; SHIN, K. Y. Black phosphorus-based smart electrorheological fluid with tailored phase transition and exfoliation. *J Ind Eng Chem.* **2020**, vol. 90, pp. 333-340.

[9] STANWAY, R.; SPROSTON, J. L.; ELWAHED, A. K. Applications of electro-rheological fluids in vibration control: A survey. *Smart Materials & Structures.* **1996**, vol. 5, no. 4, pp. 464-482.

[10] LEE, S.; KIM, Y. K.; HONG, J. Y.; JANG, J. Electro-response of MoS2 nanosheets-based smart fluid with tailorable electrical conductivity. *ACS Appl Mater Interfaces.* **2016**, vol. 8, no. 36, pp. 24221-24229.

[11] SEDLACIK, M.; MRLIK, M.; PAVLINEK, V.; KOZAKOVA, Z.; SAHA, P. Electrorheological behaviour under oscillatory shear of TiO2 rod-like particles prepared via microwave-assisted molten-salt synthesis. In: Unal H. I., editor. *13th International Conference on Electrorheological Fluids and Magnetorheological Suspensions.* Journal of Physics Conference Series. vol. 412. Bristol: Iop Publishing Ltd; **2013**. 012002.

[12] MRLIK, M.; PAVLINEK, V.; SAHA, P.; QUADRAT, O. Electrorheological properties of suspensions of polypyrrole-coated titanate nanorods. *Appl Rheol*. **2011**, vol. 21, no. 5, 52365.

[13] NOH, J.; YOON, C. M.; JANG, J. Enhanced electrorheological activity of polyaniline coated mesoporous silica with high aspect ratio. *J Colloid Interface Sci*. **2016**, vol. 470, pp. 237-244.

[14] WU, J. H.; SONG, Z. Y.; LIU, F. H.; GUO, J. J.; CHENG, Y. C.; MA, S. Q.; et al. Giant electrorheological fluids with ultrahigh electrorheological efficiency based on a micro/nano hybrid calcium titanyl oxalate composite. *NPG Asia Mater*. **2016**, vol. 8, e322.

[15] MA, N.; DONG, X. F. Effect of carrier liquid on electrorheological performance and stability of oxalate group-modified TiO2 suspensions. *J Wuhan Univ Technol-Mat Sci Edit*. **2017**, vol. 32, no. 4, pp. 854-861.

[16] GONG, X. Q.; WU, J. B.; HUANG, X. X.; WEN, W. J.; SHENG, P. Influence of liquid phase on nanoparticle-based giant electrorheological fluid. *Nanotechnology*. **2008**, vol. 19, no. 16, 165602.

[17] MRLIK, M.; PAVLINEK, V.; CHENG, Q. L.; SAHA, P. Synthesis of titanate/polypyrrole composite rod-like particles and the role of conducting polymer on electrorheological efficiency. *Int J Mod Phys B*. **2012**, vol. 26, no. 2, 1250007.

[18] HAO, T. Electrorheological suspensions. *Adv Colloid Interface Sci*. **2002**, vol. 97, no. 1-3, pp. 1-35.

[19] LIU, Y. D.; QUAN, X.; HWANG, B.; KWON, Y. K.; CHOI, H. J. Core-shell-structured monodisperse copolymer/silica particle suspension and its electrorheological response. *Langmuir*. **2014**, vol. 30, no. 7, pp. 1729-1734.

[20] DENG, Z. X.; ZHENG, L.; LI, Y. N.; DENG, X. D. *Fabrication of Al2O3/TiO2 composite particles and their ER properties*. Dai Z. D.; Qiu J. H.; Liang D., editors. Beijing: China Aviation Industry Press; **2004**. pp. 375-379.

[21] ZAID, H. M.; ADIL, M.; CHUAN, L. K.; LATIFF, N. R. A. Stability and electrorheology of ZnO nanofluids in the presence of anionic surfactants. In: Bhat A. H.; Yahya N. B.; Ramli A. R.; Soleimani H.; Zakariah S. B.; Faye I., et al., editors. *Proceeding of the 4th International Conference of Fundamental and Applied Sciences 2016*. AIP Conference Proceedings. vol. 1787. Melville: Amer Inst Physics; **2016**. 050007.

[22] FENG, P.; WAN, Q.; FU, X. Q.; WANG, T. H.; TIAN, Y. Anomalous electrorheological behavior of ZnO nanowires. *Appl Phys Lett*. **2005**, vol. 87, no. 3, 033114.

[23] HONG, T.; ZHAO, X. P.; SHU, L. Design and performance research of an adaptive damper composed of electrorheological fluids and piezoelectric ceramics. *Smart Mater Struct*. **2003**, vol. 12, no. 3, pp. 347-354.

[24] LIU, Y. D.; FANG, F. F.; CHOI, H. J. Silica nanoparticle decorated conducting polyaniline fibers and their electrorheology. *Mater Lett*. **2010**, vol. 64, no. 2, pp. 154-156.

[25] YOON, C. M.; JANG, Y.; NOH, J.; KIM, J.; LEE, K.; JANG, J. Enhanced electrorheological performance of mixed silica nanomaterial geometry. *ACS Appl Mater Interfaces*. **2017**, vol. 9, no. 41, pp. 36358-36367.

[26] LEE, C. J.; CHOI, H. J. Fabrication of poly(o-anisidine) coated silica core-shell microspheres and their electrorheological response. *Mater Res Express*. **2017**, vol. 4, no. 11, 116310.

[27] MARINS, J. A.; SOARES, B. G. Ionic liquid-based organically modified silica for the development of new electrorheological fluids. *Colloid Surf A-Physicochem Eng Asp*. **2017**, vol. 529, no., pp. 311-319.

[28] HE, K.; WEN, Q. K.; WANG, C. W.; WANG, B. X.; YU, S. S.; HAO, C. C.; et al. The preparation and electrorheological behavior of bowl-like titanium oxide nanoparticles. *Soft Matter*. **2017**, vol. 13, no. 41, pp. 7677-7688.

[29] HE, K.; WEN, Q. K.; WANG, C. W.; WANG, B. X.; YU, S. S.; HAO, C. C.; et al. Synthesis of anatase TiO2 with exposed (100) facets and enhanced electrorheological activity. *Soft Matter*. **2017**, vol. 13, no. 43, pp. 7879-7889.

[30] HE, K.; WEN, Q. K.; WANG, C. W.; WANG, B. X.; YU, S. S.; HAO, C. C.; et al. Porous TiO2 nanoparticles derived from titanium metal-organic framework and its improved electrorheological performance. *Ind Eng Chem Res*. **2018**, vol. 57, no. 20, pp. 6888-6896.

[31] LI, L. Z.; GAO, S. J. Polyaniline (PANI) and BaTiO3 composite nanotube with high suspension performance in electrorheological fluid. *Mater Today Commun*. **2020**, vol. 24, 100993.

[32] WANG, J. Y.; ZHAO, X. Y.; LIU, Y. P.; QIAN, L. X.; YAO, L.; XING, X. Q.; et al. Small-angle X-ray scattering study on the orientation of suspended sodium titanate nanofiber induced by applied electric field. *Radiat Detect Technol Methods*. **2019**, vol. 3, no. 3, 36.

[33] ALMAJDALAWI, S.; PAVLINEK, V.; MRLIK, M.; CHENG, Q.; SEDLACIK, M. Synthesis and electrorheological effect of Cr doped TiO2 nanorods with nanocavities in silicone oil suspensions. In: Unal H. I., editor. *13th International Conference on Electrorheological Fluids and Magnetorheological Suspensions*. Journal of Physics Conference Series. vol. 412. Bristol: Iop Publishing Ltd; **2013**. 012003.

[34] RAMOS-TEJADA, M. D.; RODRIGUEZ, J. M.; DELGADO, A. V. Electrorheology of clay particle suspensions. Effects of shape and surface treatment. *Rheol Acta*. **2018**, vol. 57, no. 5, pp. 405-413.

[35] PREKAS, K.; SHAH, T.; SOIN, N.; RANGOUSSI, M.; VASSILIADIS, S.; SIORES, E. Sedimentation behaviour in electrorheological fluids based

suspensions of zeolite particles in silicone oil. *J Colloid Interface Sci*. **2013**, vol. 401, pp. 58-64.

[36] ZHU, X. Y.; ZHAO, Q.; ZHANG, T.; PANG, X. F. Electrorheological response of novel polyaniline-Fe2O3 nanocomposite particles. *Polym-Plast Tech Mater*. **2019**, vol. 58, no. 5, pp. 573-577.

[37] TIAN, X. L.; YIN, Y. C.; WANG, B. X.; SONG, X. F.; SUN, S. S.; YU, S. S.; et al. Anisotropic alpha-Fe2O3@TiO2 core-shell nanoparticles and their smart electrorheological response. *Eur J Inorg Chem*. **2015**, vol., no. 3, pp. 430-440.

[38] LI, C. H.; HE, K.; SUN, W. J.; WANG, B. X.; YU, S. S.; HAO, C. C.; et al. Synthesis of hollow TiO2 nanobox with enhanced electrorheological activity. *Ceram Int*. **2020**, vol. 46, no. 10, pp. 14573-14582.

[39] QUADRAT, O.; STEJSKAL, J. Polyaniline in electrorheology. *J Ind Eng Chem*. **2006**, vol. 12, no. 3, pp. 352-361.

[40] STENICKA, M.; PAVLINEK, V.; SAHA, P.; BLINOVA, N. V.; STEJSKAL, J.; QUADRAT, O. The electrorheological efficiency of polyaniline particles with various conductivities suspended in silicone oil. *Colloid Polym Sci*. **2009**, vol. 287, no. 4, pp. 403-412.

[41] DONG, Y. Z.; CHOI, H. J. Electrorheological characteristics of poly(diphenylamine)/magnetite composite-based suspension. *Materials*. **2019**, vol. 12, no. 18, pp. 2911.

[42] STEJSKAL, J.; BOBER, P.; TRCHOVA, M.; HORSKY, J.; WALTEROVA, Z.; FILIPPOV, S. K.; et al. Oxidation of pyrrole with p-benzoquinone to semiconducting products and their application in electrorheology. *New J Chem*. **2018**, vol. 42, no. 12, pp. 10167-10176.

[43] KIM, Y. D.; SONG, I. C. Electrorheological and dielectric properties of polypyrrole dispersions. *J Mater Sci*. **2002**, vol. 37, no. 23, pp. 5051-5055.

[44] HAN, W. J.; LEE, J. H.; CHOI, H. J. Poly(diphenylamine)/polyaniline core/shell composite nanospheres synthesized using a reactive surfactant and their electrorheology. *Polymer*. **2020**, vol. 188, 122161.

[45] PLACHY, T.; SEDLACIK, M.; PAVLINEK, V.; TRCHOVA, M.; MORAVKOVA, Z.; STEJSKAL, J. Carbonization of aniline oligomers to electrically polarizable particles and their use in electrorheology. *Chem Eng J*. **2014**, vol. 256, pp. 398-406.

[46] GAO, C. Y.; KIM, M. H.; JIN, H. J.; CHOI, H. J. Synthesis and electrorheological response of graphene oxide/polydiphenylamine microsheet composite particles. *Polymers*. **2020**, vol. 12, no. 9, 1984.

[47] ZHANG, W. L.; CHOI, H. J. Graphene/graphene oxide: A new material for electrorheological and magnetorheological applications. *J Intell Mater Syst Struct*. **2015**, vol. 26, no. 14, pp. 1826-1835.

[48] CHEN, P. P.; CHENG, Q. Q.; WANG, L. M.; LIU, Y. D.; CHOI, H. J. Fabrication of dual-coated graphene oxide nanosheets by polypyrrole and

poly(ionic liquid) and their enhanced electrorheological responses. *J Ind Eng Chem*. **2019**, vol. 69, pp. 106-115.

[49] CHOI, K.; NAM, J. D.; KWON, S. H.; CHOI, H. J.; ISLAM, M. S.; KAO, N. Microfibrillated cellulose suspension and its electrorheology. *Polymers*. **2019**, vol. 11, no. 12, 2119.

[50] LIU, Z.; CHEN, P. P.; JIN, X.; WANG, L. M.; LIU, Y. D.; CHOI, H. J. Enhanced electrorheological response of cellulose: A double effect of modification by urea-terminated silane. *Polymers*. **2018**, vol. 10, no. 8, 867.

[51] MRLIK, M.; PAVLINEK, V.; ALMAJDALAWI, S.; SAHA, P.; BOBER, P.; STEJSKAL, J. Electrorheology of aniline-oligomer suspensions under oscillatory shear. In: Unal H. I., editor. *13th International Conference on Electrorheological Fluids and Magnetorheological Suspensions*. Journal of Physics Conference Series. vol. 412. Bristol: Iop Publishing Ltd; **2013**. 012007.

[52] STEJSKAL, J.; BOBER, P.; TRCHOVA, M.; HORSKY, J.; PILAR, J.; WALTEROVA, Z. The oxidation of aniline with p-benzoquinone and its impact on the preparation of the conducting polymer, polyaniline. *Synth Met*. **2014**, vol. 192, pp. 66-73.

[53] CHOI, K.; GAO, C. Y.; NAM, J. D.; CHOI, H. J. Cellulose-based smart fluids under applied electric fields. *Materials*. **2017**, vol. 10, no. 9, 1060.

[54] BAE, D. H.; CHOI, H. J.; CHOI, K.; NAM, D. J.; ISLAM, M. S.; KAO, N. Fabrication of phosphate microcrystalline rice husk based cellulose particles and their electrorheological response. *Carbohydr Polym*. **2017**, vol. 165, pp. 247-254.

[55] MORILLAS, J. R.; DE VICENTE, J. Magnetorheology: a review. *Soft Matter*. **2020**, vol. 16, no. 42, pp. 9614-9642.

[56] MOHAMMADI, N.; MAHJOOB, M. J.; KAFFASHI, B.; MALAKOOTI, S. An experimental evaluation of pre-yield and post-yield rheological models of magnetic field dependent smart materials. *J Mech Sci Technol*. **2010**, vol. 24, no. 9, pp. 1829-1837.

[57] FANG, F. F.; DONG, Y. Z.; CHOI, H. J. Effect of oxidants on morphology of interfacial polymerized polyaniline nanofibers and their electrorheological response. *Polymer*. **2018**, vol. 158, pp. 176-182.

[58] JANG, H. S.; KWON, S. H.; LEE, J. H.; CHOI, H. J. Facile fabrication of core-shell typed silica/poly(diphenylamine) composite microparticles and their electro-response. *Polymer*. **2019**, vol. 182, 121851.

[59] WERELEY, N. M. Nondimensional Herschel-Bulkley analysis of magnetorheological and electrorheological dampers. *J Intell Mater Syst Struct*. **2008**, vol. 19, no. 3, pp. 257-268.

[60] CHO, M. S.; CHOI, H. J.; JHON, M. S. Shear stress analysis of a semiconducting polymer based electrorheological fluid system. *Polymer*. **2005**, vol. 46, no. 25, pp. 11484-11488.

[61] HONG, C. H.; CHOI, H. J.; SEO, Y. Comment on "Transient overshoot of the electrorheological responses of conducting polymer-coated polyethylene suspensions in mineral oil". *Synth Met*. **2008**, vol. 158, no. 1-2, pp. 72-74.

[62] LIU, Y. D.; PARK, B. J.; KIM, Y. H.; CHOI, H. J. Smart monodisperse polystyrene/polyaniline core-shell structured hybrid microspheres fabricated by a controlled releasing technique and their electro-responsive characteristics. *J Mater Chem*. **2011**, vol. 21, no. 43, pp. 17396-17402.

[63] FANG, F. F.; CHOI, H. J.; CHOI, W. S. Phase transition of conducting polymer/clay nanocomposite suspensions under an electric field. *Philos Mag*. **2010**, vol. 90, no. 17-18, pp. 2507-2517.

[64] MOHAMMADI, F.; SEDAGHATI, R. Dynamic mechanical properties of an electrorheological fluid under large-amplitude oscillatory shear strain. *J Intell Mater Syst Struct*. **2012**, vol. 23, no. 10, pp. 1093-1105.

[65] MOON, I. J.; CHOI, H. J. Core-shell-structured copolyaniline-coated polymeric nanoparticle suspension and its viscoelastic response under various electric fields. *Materials*. **2015**, vol. 8, no. 8, pp. 4932-4942.

[66] PIAO, S. H.; KWON, S. H.; CHOI, H. J. Stimuli-responsive polymer-clay nanocomposites under electric fields. *Materials*. **2016**, vol. 9, no. 1, 52.

[67] SIM, B.; BAE, D. H.; CHOI, H. J.; CHOI, K.; ISLAM, M. S.; KAO, N. Fabrication and stimuli response of rice husk-based microcrystalline cellulose particle suspension under electric fields. *Cellulose*. **2016**, vol. 23, no. 1, pp. 185-197.

[68] DONG, Y. Z.; KWON, S. H.; CHOI, H. J.; PUTHIARAJ, P.; AHN, W. S. Electrorheological response of microporous covalent triazine-based polymeric particles. *Colloid Polym Sci*. **2018**, vol. 296, no. 5, pp. 907-915.

[69] JUN, C. S.; KWON, S. H.; CHOI, H. J.; SEO, Y. Polymeric nanoparticle-coated pickering emulsion-synthesized conducting polyaniline hybrid particles and their electrorheological study. *ACS Appl Mater Interfaces*. **2017**, vol. 9, no. 51, pp. 44811-44819.

[70] HAO, T.; KAWAI, A.; IKAZAKI, F. Mechanism of the electrorheological effect: Evidence from the conductive, dielectric, and surface characteristics of water-free electrorheological fluids. *Langmuir*. **1998**, vol. 14, no. 5, pp. 1256-1262.

[71] PLACHY, T.; MRLIK, M.; KOZAKOVA, Z.; SULY, P.; SEDLACIK, M.; PAVLINEK, V.; et al. The electrorheological behavior of suspensions based on molten-salt synthesized lithium titanate nanoparticles and their core-shell titanate/urea analogues. *ACS Appl Mater Interfaces*. **2015**, vol. 7, no. 6, pp. 3725-3731.

[72] YIN, J. B.; XIA, X.; ZHAO, X. P. Conductivity, polarization and electrorheological activity of polyaniline nanotubes during thermo-oxidative treatment. *Polym Degrad Stabil*. **2012**, vol. 97, no. 11, pp. 2356-2363.

[73] SHEN, R.; WANG, X. Z.; LU, Y.; WANG, D.; SUN, G.; CAO, Z. X.; et al. Polar-molecule-dominated electrorheological fluids featuring high yield stresses. *Adv Mater*. **2009**, vol. 21, no. 45, pp. 4631-4635.

[74] PLACHY, T.; SEDLACIK, M.; PAVLINEK, V.; STEJSKAL, J. The observation of a conductivity threshold on the electrorheological effect of p-phenylenediamine oxidized with p-benzoquinone. *J Mater Chem C*. **2015**, vol. 3, no. 38, pp. 9973-9980.

[75] EGORYSHEVA, A. V.; KRAEV, A. S.; GAJTKO, O. M.; BARANCHIKOV, A. E.; AGAFONOV, A. V.; IVANOV, V. K. Electrorheological fluids based on bismuth ferrites BiFeO3 and Bi2Fe4O9. *Russ J Inorg Chem*. **2020**, vol. 65, no. 8, pp. 1253-1263.

[76] YUAN, X.; ZHOU, X. F.; LIANG, Y. D.; WANG, L. J.; CHEN, R. M.; ZHANG, M. Y.; et al. A stable high-performance isotropic electrorheological elastomer towards controllable and reversible circular motion. *Compos Pt B-Eng*. **2020**, vol. 193, pp. 107988.

[77] EGORYSHEVA, A. V.; KRAEV, A. S.; GAJTKO, O. M.; KUSOVA, T. V.; BARANCHIKOV, A. E.; AGAFONOV, A. V.; et al. High electrorheological effect in Bi1.8Fe1.2SbO7 suspensions. *Powder Technol*. **2020**, vol. 360, pp. 96-103.

[78] HAVRILIA.S; NEGAMI, S. A complex plane representation of dielectric and mechanical relaxation processes in some polymers. *Polymer*. **1967**, vol. 8, no. 4, pp. 161-&.

[79] MRLIK, M.; SEDLACIK, M.; PAVLINEK, V.; BOBER, P.; TRCHOVA, M.; STEJSKAL, J.; et al. Electrorheology of aniline oligomers. *Colloid Polym Sci*. **2013**, vol. 291, no. 9, pp. 2079-2086.

[80] ZHAO, J.; LEI, Q.; HE, F.; ZHENG, C.; LIU, Y.; ZHAO, X. P.; et al. Interfacial polarization and electroresponsive electrorheological effect of anionic and cationic poly(ionic liquids). *ACS Appl Polym Mater*. **2019**, vol. 1, no. 11, pp. 2862-2874.

[81] STEJSKAL, J.; MRLIK, M.; PLACHY, T.; TRCHOVA, M.; KOVAROVA, J.; LI, Y. Molybdenum and tungsten disulfides surface-modified with a conducting polymer, polyaniline, for application in electrorheology. *React Funct Polym*. **2017**, vol. 120, pp. 30-37.

[82] SEDLACIK, M.; MRLIK, M.; KOZAKOVA, Z.; PAVLINEK, V.; KURITKA, I. Synthesis and electrorheology of rod-like titanium oxide particles prepared via microwave-assisted molten-salt method. *Colloid Polym Sci*. **2013**, vol. 291, no. 5, pp. 1105-1111.

[83] CABUK, M. Electrorheological response of mesoporous expanded perlite particles. *Microporous Mesoporous Mat*. **2017**, vol. 247, no., pp. 60-65.

[84] KIM, S. G.; LIM, J. Y.; SUNG, J. H.; CHOI, H. J.; SEO, Y. Emulsion polymerized polyaniline synthesized with dodecylbenzenesulfonic acid and its electrorheological characteristics: Temperature effect. *Polymer*. **2007**, vol. 48, no. 22, pp. 6622-6631.

[85] TANG, J.; WEN, X. H.; LIU, Z. P.; WANG, J. J.; ZHANG, P. Synthesis and electrorheological performances of 2D PANI/TiO2 nanosheets. *Colloid Surf A-Physicochem Eng Asp*. **2018**, vol. 552, pp. 24-31.

[86] DAVIS, L. C. Time-dependent and nonlinear effects in electrorheological fluids. *J Appl Phys*. **1997**, vol. 81, no. 4, pp. 1985-1991.

[87] SEO, Y. P.; CHOI, H. J.; SEO, Y. A simplified model for analyzing the flow behavior of electrorheological fluids containing silica nanoparticle-decorated polyaniline nanofibers. *Soft Matter*. **2012**, vol. 8, no. 17, pp. 4659-4663.

[88] YIN, J. B.; SHUI, Y. J.; CHANG, R. T.; ZHAO, X. P. Graphene-supported carbonaceous dielectric sheets and their electrorheology. *Carbon*. **2012**, vol. 50, no. 14, pp. 5247-5255.

[89] SHIN, K.; KIM, D.; CHO, J. C.; LIM, H. S.; KIM, J. W.; SUH, K. D. Monodisperse conducting colloidal dipoles with symmetric dimer structure for enhancing electrorheology properties. *J Colloid Interface Sci*. **2012**, vol. 374, pp. 18-24.

[90] LIU, J.; WEN, X. H.; LIU, Z. P.; TAN, Y.; YANG, S. Y.; ZHANG, P. Electrorheological performances of poly(o-toluidine) and p-toluenesulfonic acid doped poly(o-toluidine) suspensions. *Colloid Polym Sci*. **2015**, vol. 293, no. 5, pp. 1391-1400.

[91] HAO, T. *Electrorheological fluids: The non-aqueous suspensions*. 1 ed. Mobius D. M., R., editor. San Diego: Elsevier **2005**.

[92] LAPENTA, G.; MAIZZA, G.; PALMIERI, A.; BORETTO, G.; DEBENEDETTI, M. Phase transitions in electrorheological fluids using molecular dynamics simulations. *Phys Rev E*. **1999**, vol. 60, no. 4, pp. 4505-4510.

[93] YE, X. M.; KANDLIKAR, S. G.; LI, C. X. Viscosity of nanofluids containing anisotropic particles: A critical review and a comprehensive model. *Eur Phys J E*. **2019**, vol. 42, no. 12, 159.

[94] GEHIN, C.; PERSELLO, J.; CHARRAUT, D.; CABANE, B. Electrorheological properties and microstructure of silica suspensions. *J Colloid Interface Sci*. **2004**, vol. 273, no. 2, pp. 658-667.

[95] HIAMTUP, P.; SIRIVAT, A.; JAMIESON, A. M. Field strength dependence of the high-frequency viscoelastic relaxation process in polyaniline/silicone oil electrorheological suspensions. *Express Polym Lett*. **2008**, vol. 2, no. 10, pp. 688-694.

[96] OTSUBO, Y.; SEKINE, M.; KATAYAMA, S. Electrorheological properties of silica suspensions. *J Rheol*. **1992**, vol. 36, no. 3, pp. 479-496.

[97] LENGALOVA, A.; PAVLINEK, V.; SAHA, P.; STEJSKAL, J.; KITANO, T.; QUADRAT, O. The effect of dielectric properties on the electrorheology of suspensions of silica particles coated with polyaniline. *Physica A*. **2003**, vol. 321, no. 3-4, pp. 411-424.

[98]   PAVLINEK, V.; QUADRAT, O.; SAHA, P.; BENES, M. J.; TRLICA, J. Electrorheological properties of hydrolyzed poly(glycidyl methacrylate) suspensions. *Colloid Polym Sci*. **1998**, vol. 276, no. 8, pp. 690-697.

[99]   GOODWIN, J. W.; MARKHAM, G. M.; VINCENT, B. Studies on model electrorheological fluids. *J Phys Chem B*. **1997**, vol. 101, no. 11, pp. 1961-1967.

[100]   WEN, W. J.; HUANG, X. X.; YANG, S. H.; LU, K. Q.; SHENG, P. The giant electrorheological effect in suspensions of nanoparticles. *Nat Mater*. **2003**, vol. 2, no. 11, pp. 727-730.

[101]   HUANG, X. X.; WEN, W. J.; YANG, S. H.; SHENG, P. Mechanisms of the giant electrorheological effect. *Solid State Commun*. **2006**, vol. 139, no. 11-12, pp. 581-588.

[102]   LENGALOVA, A.; PAVLINEK, V.; SAHA, P.; QUADRAT, O.; STEJSKAL, J. The effect of dispersed particle size and shape on the electrorheological behaviour of suspensions. *Colloid Surf A-Physicochem Eng Asp*. **2003**, vol. 227, no. 1-3, pp. 1-8.

[103]   VINCENZI, D. Orientation of non-spherical particles in an axisymmetric random flow. *J Fluid Mech*. **2013**, vol. 719, no., pp. 465-487.

[104]   CHENG, Y. C.; GUO, J. J.; LIU, X. H.; SUN, A. H.; XU, G. J.; CUI, P. Preparation of uniform titania microspheres with good electrorheological performance and their size effect. *J Mater Chem*. **2011**, vol. 21, no. 13, pp. 5051-5056.

[105]   MCINTYRE, E. C.; YANG, H. X.; GREEN, P. F. Electrorheology of polystyrene filler/polyhedral silsesquioxane suspensions. *ACS Appl Mater Interfaces*. **2012**, vol. 4, no. 4, pp. 2148-2153.

[106]   LEE, S. Highly uniform silica nanoparticles with finely controlled sizes for enhancement of electro-responsive smart fluids. *J Ind Eng Chem*. **2019**, vol. 77, pp. 426-431.

[107]   AHN, B. G.; CHOI, U. S.; KWON, O. K. Electrorheological properties of phosphoric ester cellulose electrorheological suspensions at elevated temperatures. *Polym J*. **2000**, vol. 32, no. 6, pp. 476-480.

[108]   PAN, J. L.; JIN, X.; ZHANG, Z. L.; WANG, L. M.; LIU, Y. D.; CHOI, H. J. Temperature-dependent electrorheology of a suspension based on copolymeric P(NIPAM-co- AMIm Cl) colloidal particles. *Smart Mater Struct*. **2020**, vol. 29, no. 12, 124001.

[109]   MORATO, M. M.; PHAM, T. P.; SENAME, O.; DUGARD, L. Development of a simple ER damper model for fault-tolerant control design. *J Braz Soc Mech Sci Eng*. **2020**, vol. 42, no. 10, 502.

[110]   VIVAS-LOPEZ, C. A.; HERNANDEZ-ALCANTARA, D.; MORALES-MENENDEZ, R.; RAMIREZ-MENDOZA, R. A.; AHUETT-GARZA, H. Method for modeling electrorheological dampers using its dynamic characteristics. *Math Probl Eng*. **2015**, vol. 2015, 905731.

[111] PAPADOPOULOS, C. A. Brakes and clutches using ER fluids. *Mechatronics*. **1998**, vol. 8, no. 7, pp. 719-726.

[112] MUSIALEK, I.; KESY, Z.; KESY, A.; KIM, G. W.; CHOI, S. B. Mathematical modelling and experimental validation of a hybrid clutch combined with two modes: hydraulic and electrorheological fluid modes. *Smart Mater Struct*. **2021**, vol. 30, no. 1, pp. 017002.

[113] MUSIALEK, I.; MIGUS, M.; OLSZAK, A.; OSOWSKI, K.; KESY, Z.; KESY, A.; et al. Analysis of a combined clutch with an electrorheological fluid. *Smart Mater Struct*. **2020**, vol. 29, no. 8, pp. 087006.

[114] TAN, A. S.; BELKNER, J.; STROSCHKE, A.; SATTEL, T. Damping adjustment utilizing digital electrorheological valves with parallely segmented electrodes. *Smart Mater Struct*. **2019**, vol. 28, no. 7, 075013.

[115] SIMMONDS, A. J. Electrorheological valves in a hydraulic circuit. *Iee Proceedings-D Control Theory and Applications*. **1991**, vol. 138, no. 4, pp. 400-404.

[116] KAMELREITER, M.; KEMMETMULLER, W.; KUGI, A. Digitally controlled electrorheological valves and their application in vehicle dampers. *Mechatronics*. **2012**, vol. 22, no. 5, pp. 629-638.

[117] CHOI, S. B.; LEE, D. Y. Rotational motion control of a washing machine using electrorheological clutches and brakes. *Proc Inst Mech Eng Part C-J Eng Mech Eng Sci*. **2005**, vol. 219, no. 7, pp. 627-637.

[118] MONKMAN, G. J.; BOESE, H.; ERMERT, H.; KLEIN, D.; FREIMUTH, H.; BAUMANN, M.; et al. Technologies for haptic systems in telemedicine. In: Nerlich M.; Schaechinger U., editors. *Integration of Health Telematics into Medical Practice*. Studies in Health Technology and Informatics. vol. 97. Amsterdam: Ios Press; **2003**. pp. 83-93.

[119] LIU, Y. D.; LEE, B. M.; PARK, T. S.; KIM, J. E.; CHOI, H. J.; BOOH, S. W. Optically transparent electrorheological fluid with urea-modified silica nanoparticles and its haptic display application. *J Colloid Interface Sci*. **2013**, vol. 404, pp. 56-61.

[120] BISWAS, S.; VISELL, Y. Emerging material technologies for haptics. *Adv Mater Technol*. **2019**, vol. 4, no. 4, 1900042.

[121] BOHON, K.; KRAUSE, S. An electrorheological fluid and siloxane gel based electromechanical actuator: Working toward an artificial muscle. *J Polym Sci Pt B-Polym Phys*. **1998**, vol. 36, no. 6, pp. 1091-1094.

[122] NIKITCZUK, J.; WEINBERG, B.; CANAVAN, P. K.; MAVROIDIS, C. Active knee rehabilitation orthotic device with variable damping characteristics implemented via an electrorheological fluid. *IEEE-ASME Trans Mechatron*. **2010**, vol. 15, no. 6, pp. 952-960.

[123] DAVIDSON, J. R.; KREBS, H. I. An electrorheological fluid actuator for rehabilitation robotics. *IEEE-ASME Trans Mechatron*. **2018**, vol. 23, no. 5, pp. 2156-2167.

[124] BROOKFIELD, D. J.; DLODLO, Z. B. Robot torque and position control using an electrorheological actuator. *Proc Inst Mech Eng Part I-J Syst Control Eng*. **1998**, vol. 212, no. I3, pp. 229-238.

[125] CHETRAN, B.; JISA, S.; MANDRU, D. Resistive torques in rehabilitation engineering equipment. In: Pisla D.; Bleuler H.; Rodic A.; Vaida C.; Pisla A., editors. *New Trends in Medical and Service Robot: Theory and Integrated Applications*. Mechanisms and Machine Science. vol. 16. Berlin: Springer-Verlag Berlin; **2014**. pp. 43-55.

[126] KOROBKO, E. V.; NOVIKOVA, Z. A. Features of the mechanisms of conductivity of the electrorheological fluids with double doped tio2 particles under external temperature effects. *Front Mater*. **2019**, vol. 6, 132.

[127] PLACHY, T.; KUTALKOVA, E.; SEDLACIK, M.; VESEL, A.; MASAR, M.; KURITKA, I. Impact of corrosion process of carbonyl iron particles on magnetorheological behavior of their suspensions. *J Ind Eng Chem*. **2018**, vol. 66, pp. 362-369.

[128] WENDT, E.; BUSING, K. W. A new type of hydraulic actuator using electrorheological fluids. *Int J Mod Phys B*. **1999**, vol. 13, no. 14-16, pp. 2176-2182.

[129] DONG, Y. Z.; CHOI, K.; KWON, S. H.; NAM, J. D.; CHOI, H. J. Nanoparticles functionalized by conducting polymers and their electrorheological and magnetorheological applications. *Polymers*. **2020**, vol. 12, no. 1, 204.

[130] EROL, O.; UNAL, H. I. Core/shell-structured, covalently bonded TiO2/poly(3,4-ethylenedioxythiophene) dispersions and their electrorheological response: the effect of anisotropy. *RSC Adv*. **2015**, vol. 5, no. 125, pp. 103159-103171.

[131] SEDLACIK, M.; MRLIK, M.; PAVLINEK, V.; SAHA, P.; QUADRAT, O. Electrorheological properties of suspensions of hollow globular titanium oxide/polypyrrole particles. *Colloid Polym Sci*. **2012**, vol. 290, no. 1, pp. 41-48.

[132] LIANG, Y. D.; YUAN, X.; WANG, L. J.; ZHOU, X. F.; REN, X. J.; HUANG, Y. F.; et al. Highly stable and efficient electrorheological suspensions with hydrophobic interaction. *J Colloid Interface Sci*. **2020**, vol. 564, pp. 381-391.

[133] SEDLACIK, M.; PAVLINEK, V. A tensiometric study of magnetorheological suspensions' stability. *RSC Adv*. **2014**, vol. 4, no. 102, pp. 58377-58385.

[134] ZHANG, K.; LI, H. T.; DONG, Y. Z.; ZHANG, H. L.; ZHAO, W.; ZHAO, S. Q.; et al. Jellyfish-shaped p-phenylenediamine functionalized graphene oxide-g-polyaniline fibers and their electrorheology. *Polymer*. **2019**, vol. 168, pp. 29-35.

[135] KUTALKOVA, E.; MRLIK, M.; ILCIKOVA, M.; OSICKA, J.; SEDLACIK, M.; MOSNACEK, J. Enhanced and tunable electrorheological

capability using surface initiated atom transfer radical polymerization modification with simultaneous reduction of the graphene oxide by silyl-based polymer grafting. *Nanomaterials*. **2019**, vol. 9, no. 2, 308.

[136] HONG, S.; KIM, M.; HONG, C. K.; JUNG, D.; SHIM, S. E. Encapsulation of multi-walled carbon nanotubes by poly(4-vinylpyridine) and its dispersion stability in various solvent media. *Synth Met*. **2008**, vol. 158, no. 21-24, pp. 900-907.

[137] CVEK, M.; MRLIK, M.; MOUCKA, R.; SEDLACIK, M. A systematical study of the overall influence of carbon allotrope additives on performance, stability and redispersibility of magnetorheological fluids. *Colloid Surf A-Physicochem Eng Asp*. **2018**, vol. 543, pp. 83-92.

[138] PLACHY, T.; CVEK, M.; MUNSTER, L.; HANULIKOVA, B.; SULY, P.; VESEL, A.; et al. Enhanced magnetorheological effect of suspensions based on carbonyl iron particles coated with poly(amidoamine) dendrons. *Rheol Acta*. **2021**, vol. 60, no. 5, pp. 263-276.

[139] CHENG, Q. L.; PAVLINEK, V.; HE, Y.; YAN, Y. F.; LI, C. Z.; SAHA, P. Synthesis and electrorheological characteristics of sea urchin-like TiO2 hollow spheres. *Colloid Polym Sci*. **2011**, vol. 289, no. 7, pp. 799-805.

[140] JI, X. Q.; ZHANG, W. L.; JIA, W. P.; WANG, X. X.; TIAN, Y.; DENG, L.; et al. Cactus-like double-shell structured SiO2@TiO2 microspheres: Fabrication, electrorheological performances and microwave absorption. *J Ind Eng Chem*. **2017**, vol. 56, pp. 203-211.

[141] SUN, W. J.; ZHENG, H. N.; CHEN, Y.; LI, C. H.; WANG, B. X.; HAO, C. C.; et al. Preparation and electrorheological properties of peanut-like hollow core-shell structure TiO2@SiO2 nanoparticles. *Adv Eng Mater*. **2021**, 2001416.

[142] ZHANG, W. L.; JIANG, D.; WANG, X. X.; HAO, B. N.; LIU, Y. D.; LIU, J. Q. Growth of polyaniline nanoneedles on MoS2 nanosheets, tunable electroresponse, and electromagnetic wave attenuation analysis. *J Phys Chem C*. **2017**, vol. 121, no. 9, pp. 4989-4998.

[143] ZHANG, Z. L.; ZHANG, Z. G.; HAO, B. N.; ZHANG, H. Y.; WANG, M.; LIU, Y. D. Fabrication of imidazolium-based poly(ionic liquid) microspheres and their electrorheological responses. *J Mater Sci*. **2017**, vol. 52, no. 10, pp. 5778-5787.

[144] XIA, M. Y.; NIE, J. H.; ZHANG, Z. L.; LU, X. M.; WANG, Z. L. Suppressing self-discharge of supercapacitors via electrorheological effect of liquid crystals. *Nano Energy*. **2018**, vol. 47, pp. 43-50.

[145] MIYOSHI, T.; YOSHIDA, K.; KIM, J. W.; EOM, S. I.; YOKOTA, S. An MEMS-based multiple electro-rheological bending actuator system with an alternating pressure source. *Sens Actuator A-Phys*. **2016**, vol. 245, pp. 68-75.

[146] KUTALKOVA, E.; PLACHY, T.; OSICKA, J.; CVEK, M.; MRLIK, M.; SEDLACIK, M. Electrorheological behavior of iron(ii) oxalate micro-rods. *RSC Adv*. **2018**, vol. 8, no. 44, pp. 24773-24779.

[147] DONG, X. F.; HUO, S.; QI, M. Comparison of electrorheological performance between urea-coated and graphene oxide-wrapped core-shell structured amorphous TiO2 nanoparticles. *Smart Mater Struct*. **2016**, vol. 25, no. 1, 015033.

[148] MA, N.; NIU, C. G.; DONG, X. F.; HAN, B. G. Electrorheological properties of carbon nanotube decorated TiO2 nanoparticles. *Mater Res Express*. **2017**, vol. 4, no. 6, 065701.

[149] KUTALKOVA, E.; RONZOVA, A.; OSICKA, J.; SKODA, D.; SEDLACIK, M. Influence of synthesis conditions on electrorheological performance of iron(II) oxalate. *J Ind Eng Chem*. **2021**, Paper accepted, published online on 16th of May.

[150] KUTALKOVA, E.; PLACHY, T.; SEDLACIK, M. On the enhanced sedimentation stability and electrorheological performance of intelligent fluids based on sepiolite particles. *J Mol Liq*. **2020**, vol. 309, 113120.

[151] YIN, J. B.; WANG, X. X.; CHANG, R. T.; ZHAO, X. P. Polyaniline decorated graphene sheet suspension with enhanced electrorheology. *Soft Matter*. **2012**, vol. 8, no. 2, pp. 294-297.

[152] MRLIK, M.; ILCIKOVA, M.; PLACHY, T.; MOUCKA, R.; PAVLINEK, V.; MOSNACEK, J. Tunable electrorheological performance of silicone oil suspensions based on controllably reduced graphene oxide by surface initiated atom transfer radical polymerization of poly(glycidyl methacrylate). *J Ind Eng Chem*. **2018**, vol. 57, pp. 104-112.

LIST OF FIGURES

LIST OF TABLES

LIST OF SYMBOLS AND ABREVIATIONS

α, β	shape parameters	[–]
$\dot{\gamma}$	shear rate	[s^{-1}]
γ	strain	[–]
$\Delta\varepsilon'$	dielectric relaxation strength	[–]
ε'	relative permittivity	[–]
ε''	dielectric loss factor	[–]
ε'_0	relative permittivity at zero frequency	[–]
ε'_∞	relative permittivity at infinitely frequency	[–]
$\varepsilon^*_{(\omega)}$	complex permittivity	[–]
ε_0	permittivity of free space	[F·m^{-1}]
ε_c	relative permittivity of continuous phase	[–]
ε_p	relative permittivity of dispersed particles	[–]
ε_{lm}	relative permittivity of liquid medium	[–]
η	shear viscosity	[Pa·s]
η_c	viscosity of continuous phase	[Pa·s]
η_0	viscosity in the absence of an electric field	[Pa·s]
η_E	viscosity in the presence of an electric field	[Pa·s]
η_{pl}	plastic viscosity	[Pa·s]
η_∞	shear viscosity at high shear rates	[Pa·s]
λ	polarization interaction parameter	[–]
σ_p	conductivity of the solid phase	[S·m^{-1}]
σ_{lm}	conductivity of the liquid phase	[S·m^{-1}]
τ	shear stress	[Pa]
τ_y	yield stress	[Pa]
ω	angular frequency	[rad·s^{-1}]
D	diameter	[m]
E	electric field	[V·mm^{-1}]
f	frequency	[Hz]
G^*	complex shear modulus	[Pa]
G'	storage modulus	[Pa]
G''	loss modulus	[Pa]
K	consistency index	[Pa·s^n]
L	length	[m]
L/D	aspect ratio	[–]
ΔM	dielectric relaxation strength	[–]
M_∞	unrelaxed dielectric modulus	[–]
$M^*_{HN}(\omega)$	the complex dielectric modulus	[–]
M_n	Mason number	[–]
n	Newtonian index	[–]

| Pe | Peclet number | $[-]$ |
| t_1, t_2 | time constants | $[s]$ |

1D	one-dimensional	
2D	two-dimensional	
CCJ	Cho–Choi–Jhon model	
ER	electrorheological	
ERFs	electrorheological fluids	
Fe_3O_4	iron(II,III) oxide	
$FeC_2O_4 \cdot 2H_2O$	iron(II) oxalate dihydrate	
GER	giant electrorheological fluids	
GO	graphene oxide	
HEMATMS	2-(trimethylsilyloxy)ethyl methacrylate	
H–N	Havriliak–Negami model	
MoS_2	molybdenum disulfide	
OX	iron(ii) oxalate	
PANI	polyaniline	
PPy	polypyrrole	
SiO_2	silica	
SI-ATRP	surface-initiated atom transfer radical polymerization	
TiO_2	titanium dioxide	

CURRICULUM VITAE

Personal information

Surname and name	Kutálková Erika
Address	U Hřiště 40, 763 64 Spytihněv, Czech Republic
Telephone	+420 608 636 221
E-mail	ekutalkova@utb.cz
Nationality	Czech
Date of Birth	11/02/1992

Work Experience

Dates	2017 – present
Occupation or Position Held	Research assistant
Name of Employer	Tomas Bata University in Zlín, Centre of Polymer Systems

Education

Dates	2017 – present
Title of Qualification Awarded	Doctoral Study – Expected defense in 09/2021
Principal Branch	Nanotechnology and Advanced Materials
Organization Providing	Tomas Bata University in Zlín, Centre of Polymer Systems
Dates	2015 – 2017
Title of Qualification Awarded	Ing. eq. M.Sc.
Principal Branch	Polymer Engineering
Organization Providing	Tomas Bata University in Zlín, Faculty of Technology
Dates	2012 – 2015
Title of Qualification Awarded	Bc.
Principal Branch	Polymeric Materials and Technology
Organization Providing	Tomas Bata University in Zlín, Faculty of Technology

Training Abroad

Dates	October – November 2020
	Student traineeship at Johannes Kepler University Linz, Institute of Polymer Sciences (Austria)
Field of Study	Injection-molding of magnetorheological elastomers

Expertise	
Fields	electrorheology, magnetorheology, rheology, polymer processing

Other Languages	Level
English	B2
French	A1

LIST OF PUBLICATIONS

Publications in the Journals with Impact Factor:

[1]   KUTALKOVA, E.; RONZOVA, A.; OSICKA, J.; SKODA, D.; SEDLACIK, M. Influence of synthesis conditions on electrorheological performance of iron(II) oxalate. *J Ind Eng Chem.* **2021**, Paper accepted, published online on 16th of May.

[2]   CVEK, M.; KUTALKOVA, E.; MOUCKA, R.; URBANEK, P.; SEDLACIK, M. Lightweight, transparent piezoresistive sensors conceptualized as anisotropic magnetorheological elastomers: A durability study. *Int. J. Mech. Sci.* **2020**, vol. 183, 105816.

[3]   DURPEKOVA, S.; FILATOVA, K.; CISAR, J.; RONZOVA, A.; KUTALKOVA, E.; SEDLARIK, V. A Novel Hydrogel Based on Renewable Materials for Agricultural Application. *Int J Polym Sci.* **2020**, vol. 2020, 8363418.

[4]   KUTALKOVA, E.; PLACHY, T.; SEDLACIK, M. On the enhanced sedimentation stability and electrorheological performance of intelligent fluids based on sepiolite particles. *J Mol Liq.* **2020**, vol. 309, 113120.

[5]   PLACHY, T.; MASAR, M.; MRLIK, M.; MACHOVSKY, M.; MACHOVSKA, Z.; KUTALKOVA, E.; et al. Switching between negative and positive electrorheological effect of g-C_3N_4 by copper ions doping. *Adv Powder Technol.* **2019**, vol. 30, no. 4, pp. 714-723.

[6]   KUTALKOVA, E.; MRLIK, M.; ILCIKOVA, M.; OSICKA, J.; SEDLACIK, M.; MOSNACEK, J. Enhanced and Tunable Electrorheological Capability using Surface Initiated Atom Transfer Radical Polymerization Modification with Simultaneous Reduction of the Graphene Oxide by Silyl-Based Polymer Grafting. *Nanomaterials.* **2019**, vol. 9, no. 2, 308.

[7]   MRLIK, M.; ILCIKOVA, M.; OSICKA, J.; KUTALKOVA, E.; MINARIK, A.; et al. Electrorheology of SI-ATRP-modified graphene oxide particles with poly(butyl methacrylate): effect of reduction and compatibility with silicone oil. *RSC Adv.* **2019**, vol. 9, no. 3, pp. 1187-1198.

[8]   PLACHY, T.; KUTALKOVA, E.; SEDLACIK, M.; VESEL, A.; MASAR, M.; KURITKA, I. Impact of corrosion process of carbonyl iron particles on

magnetorheological behavior of their suspensions. *J Ind Eng Chem*. **2018**, vol. 66, pp. 362-369.

[9]   KUTALKOVA, E.; PLACHY, T.; OSICKA, J.; CVEK, M.; MRLIK, M.; SEDLACIK, M. Electrorheological behavior of iron(II) oxalate micro-rods. *RSC Adv*. **2018**, vol. 8, no. 44, pp. 24773-24779.

Original Full Papers in Conference Proceedings (Indexed on Web of Science):

[1]   MOUCKA, R.; SEDLACIK, M.; KUTALKOVA, E. Magnetorheological Elastomers: Electric properties versus microstructure. Recent Advances on Environment, Chemical Engineering and Materials; AIP Conference Proceedings, **2018**, vol. 2022, 020017-1.

Conference Contribution:

[1]   OSICKA, J.; CVEK, M.; KUTALKOVA, E.; MOUCKA, R.; SEDLACIK, M. Magnetorheological elastomers as a lightweight, transparent piezoresistive sensor. In: *ERMR 2019 – International Conference on Electrorheological Fluids and Magnetorheorogical Suspension*s, (ed. Li, W.), **2019**, Wollongong, Australia.

[2]   KUTALKOVA, E.; PLACHY, T.; SEDLACIK, M. Electrorheological fluid based on cellulose particles: optimization of measuring procedure. In: *4rd International Conference on Rheology and Modelling of Materials*, (ed. Gömze, L. A.), **2019**, Miskolcs-Lillafüred, Hungary.

[3]   SEDLACIK, M.; MOUCKA, R.; KUTALKOVA, E.; CVEK, M.; BILEK, O. Effect of Percolation Threshold on the Piezo-Resistive Behavior of Magnetorheological Elastomers. In: *4rd International Conference on Rheology and Modelling of Materials*, (ed. Gömze, L. A.), **2019**, Miskolcs-Lillafüred, Hungary.

[4]   KUTALKOVA, E.; PLACHY, T.; OSICKA, J.; CVEK, M.; SEDLACIK, M. Iron(II) oxalate micro-rods as a promising material for electrorheology. In: *Polymers: Site of Advanced Horizons and Ambits*, (ed. Hausnerova, B.), **2018**, Zlín, Czech Republic.

[5]   KUTALKOVA, E.; MRLIK, M.; ILCIKOVA, M.; OSICKA, J.; SEDLACIK, M.; MOSNACEK, J. Grafting of the poly[2-(trimethylsilyloxy)ethyl methacrylate] from the graphene oxide by SI-ATRP technique leading towards improved wettability, sedimentation stability and electrorheological performance. In: *ERMR 2018 - International Conference on Electrorheological Fluids and Magnetorheological Suspensions*, (ed. Wereley, N. M.), **2018**, College Park, Maryland, USA.

[6]   PLACHY, T.; KUTALKOVA, E.; MRLIK, M. Influence of polyhedral oligomeric silsesquioxane particles on the thermomechanical behaviour of epoxy resin. In: *3rd International Conference on Rheology and Modelling of Materials*, (ed. Gömze, L. A.), **2017**, Miskolcs-Lillafüred, Hungary.

[7]   CVEK, M.; PLACHY, T.; OSICKA, J.; KUTALKOVA, E.; MRLIK, M.; SEDLACIK, M. Ferrous oxalate micro-rods as a promising material for electrorheology. In: *3rd International Conference on Rheology and Modelling of Materials*, (ed. Gömze, L. A.), **2017**, Miskolcs-Lillafüred, Hungary.

WORK ON PROJECTS

Project	Period	Position
Internal Grant Agency of TBU in Zlín, *Piezoresistivity of advanced materials*, IGA/CPS/2021/003	2021	Member of research team
Development project, *Smart nanomaterials: from basics to application*, RP/CPS/2020/006	2021	Member of research team
Internal Grant Agency of TBU in Zlín, *Influence of Modifications Dispersion Particles on the Utility Properties of Magnetorheological Systems*, IGA/CPS/2020/006	2020	Principal investigator
Ministry of Agriculture of the Czech Republic, *Environmentally friendly materials for the intensification of crop production with soil protection properties based on renewable resources*, QK1910392	2020	Member of research team
Internal Grant Agency of TBU in Zlín, *Influence of organic materials on the efficiency of intelligent systems*, GA/CPS/2019/005	2019	Member of research team
Czech Science Foundation (GACR), *Novel Magnetorheological Elastomers Based on Modified Magnetic Fillers*, GA17-24730S	2017-2019	Member of research team
Internal Grant Agency of TBU in Zlín, *Preparation and characterization of electrorheological suspensions based on ferrous oxalates and clays*, IGA/CPS/2018/004	2018	Member of research team
Czech Science Foundation (GACR), *Smart systems based on modified graphene oxide particles*, GJ16-20361Y	2017-2018	Member of research team
Internal Grant Agency of TBU in Zlín, *Evaluation of Carbon-Based Nano-Additives' Influence on Magnetorheological Performance and Preparation of Electrorheological Suspension with Enhanced Sedimentation Stability*, IGA/CPS/2017/004	2017	Member of research team

Erika Kutálková

Intelligent Electrorheological Fluids

Inteligentní elektroreologické tekutiny

Doctoral Thesis Summary